DYNAMIC TESTING WITH PRE-CRASH ACTIVATION TO DESIGN ADAPTIVE SAFETY SYSTEMS

Kai-Ulrich Machens
Lars Kübler
ZF Automotive Germany GmbH, Industriestr. 20, 73553 Alfdorf
Germany

Paper Number 23-0067

ABSTRACT

Pre-crash occupant dynamics change more and more with the broad usage of advanced driver assistance systems (ADAS) and automated driving (AD) functions. Occupant interaction with pre-crash activated seatbelt systems (SBS) represent a challenge and an opportunity at the same time for providing restraint solutions tailored to the individual passenger and to the actual driving situation. To fully understand the dynamics, and to design robust control parameters, the increased complexity can eventually only be assessed by means of a virtual approach. Consequently, this requires compulsory realistic advanced physical tests and development targets to ensure that integrity and functionality of all system components are fully understood and modeled appropriately. Focusing on the most frequent crash types: frontal and rear end crashes, allows to use a specially designed, stripped-down Anthropomorphic Test Device (ATD) to dynamically load the seatbelt system in a representative way. In addition, a high-precision surrogate with different selectable upper body moments of inertia, seated on a generic steel seat with an adjustable backrest is available to extend the range of the applicable load. In both cases the retaining effect caused by friction on a real vehicle seat is accounted for by an adjustable viscous damper, retarding the motion of the lower body. These reduced setups guaranty by design a direct and accurate positioning of the ATD, minimizing test setup variability.

As a novum, a seamless transition from initial pre-crash dynamics to the final crash pulse loading can be realized when mounting these ATDs on an innovative test bench using closed-loop controlled electric linear motors to accelerate a linear ball bearing guided carbon sled along a 6-meter track for achieving a maximum in reliability and in repeatability. This physical bench test represents the foundation not only for demonstrating benefits of pre-crash activation on seat belt systems but also for validating functional SBS simulation models, so that numerical simulations become its digital twin. Reliable digital SBS simulation will be the key to generate more and advanced seat belt functions. However, the capability to measure efficiently and accurately via physical tests the performance of these SBS products throughout the entire range of their functional design space, will promote not only the product, but further raises the credibility of simulation. A new rating criterion *Characteristic Shoulder Force Level* (CFL) evaluating the SBS performance virtually is proposed, which assess the performance of the SBS intervention up to *force-closure* and demonstrates the strength of a hybrid approach. Different vehicle configurations, crash pulses, load scenarios and SBS activation strategies can be rated and directly compared to each other. This supports improved integrated safety systems solutions and allows detailed analyses of active safety pre-crash interventions as triggered by ADAS or AD. The combined virtual-physical approach is illustrated via load cases combining braking intervention with conventional and actively controlled seatbelt systems. The potential benefit to occupant safety of different combination of braking and SBS activation is measured and discussed.

INTRODUCTION

Plankermann [1] states that about 90% of all road traffic accidents can be assigned to the human factor. Full autonomous driving will eventually take the principal factor out of the equation, being the reason why this vision is so appealing in terms of road traffic safety. However, before this becomes reality, the next step forward to enhance vehicle safety is expected to be driven by new technologies in onboard sensors and electronic control units, enabling adaptive safety systems and advanced driver assistance systems (ADAS) to improve occupant real-world safety. Autonomous emergency braking (AEB), which is obligatory from 2024 for all new registered vehicles in the European Union [2], for example can help to prevent accidents, or at least reduce the severity of an accident, as described by Graci et al. [3] and the benefit of AEB for occupant safety is already acknowledged by Euro NCAP [4] and NHTSA [5].

The next safety level for occupant safety systems (OSS) will be reached when feeding back, data collected by the vehicles' surrounding and interior sensors, into an adaptive safety system for selecting the appropriate strategies and activating the protection devices accordingly, case by case. Interlinking active and passive safety allows a sooner, and case sensitive activation of the OSS, reducing the occupant injury risk.

Scenario-based verification with high accuracy bench tests

The evaluation and validation of complex case sensitive OSS functions is a challenging task since these systems must perform accordingly to all possible situations and under all possible conditions. As discussed for example by Spitzhüttl et al. [6] and

Wågström et al. [7], innovative, so-called scenario-based verification and validation approaches, combining virtual and physical testing, are considered most suitable for this task. This appreciation is also shared in the Euro NCAP Working Group paper on AEB/AES from Schramm [4], reflecting on the need to "be able to validate the OEM performance, by a combination of vehicle in the loop tests and simplified tracks". According to Reuter [8] they equally recognized within their roadmap 2030 to extend not only the number of variants of sled tests but also to incorporate virtual testing to enhance the robustness of safety system towards crash severity variance and towards occupant physis. The need for adaptive occupant safety systems is emphasized by investigations such as from Hu et al. [9]. They carried out a sensitivity study on injury risks for a wide range of the US adult population. Occupants generated from parametric human models were installed in a validated generic vehicle driver compartment and an U.S. NCAP frontal crash was simulated. Their results suggest that safety systems, that adapt to passenger stature and body shape may improve crash safety for all occupants.

The present authors addressed in [10] the need to improve on repeatability for system - or for subsystem tests to be able to identify and validate accurately functional models of seatbelt components thoroughly over the full design space. Fully validated functional models are necessary to build a reliable base to assess virtual holistic safety ratings by scenario based full vehicle simulations. For connecting physical and virtual testing they suggest in [10] to use a specifically designed test bench called Hyper Dynamic Response Actuator (HyDRA) with a generic, well defined test setup. Accurate measurement systems, enhanced control of test parameters and bench efficiency yield in reduced setup time for each test, making HyDRA the perfect tool for performing large number of load case variations, essential for the identification and validation of functional simulation models of SBS components.

The expected demand to rate and verify SBS functionality in subcomponent testing with precrash activities, motivated the development of an additional, more complex test setup on HyDRA test bench, presented in this paper, with either an ATD being accelerated under ADAS activity or under a precrash activation of an actively controlled SBS.

The chosen ATD-like kinematics to load the SBS is geared to a fundamental investigation on the influence of pre-crash activation on restraints' effectiveness. Outcome of this study is a proposition how to rate the contribution of the SBS under precrash action to real-world safety. The approach is based on the technical understanding of the classical in-crash SBS functionality which needs to be adapted to add precrash activities. An appropriate functional segmentation of the in-crash phase is presented in the next section.

CRASH PHASES FOR CLASSICAL AND INTEGRATED SAFETY

Discussions on how to mitigate the consequences of a crash, the crash sequence itself is commonly divided into three phases, the pre-crash-, the in-crash-, and the post-crash-phase, as described by Kramer et al. [11]. The shortest phase in time is the in-crash phase lasting about 100-200 ms dependent on the crash scenario, being commonly described as a velocity alignment of vehicle and occupant. Linear in-crash velocity alignment as used by Zellmer et al. [12] averages out important effects during this phase and is consequently not suited to distinguish in a meaningful way between different pretensioner systems. Voigt et al. [13] subdivide the in-crash phase, based on the shoulder belt force readings from sled tests, into the following segments: *Pretensioning – Coupling – Load Limiting*. In this paper a split of the in-crash phase into the functional segments: *crash-detection, force-closure* and *ride-down* is suggested and motivated for classical passive and integrated safety as illustrated in Figure 1, as *pretensioning* must be regarded as a sub-task to improve coupling.

Classical passive safety

The in-crash-phase in classical passive safety as depicted in Figure 1 in the upper row, starts with a constant speed situation and an occupant in its nominal position. Ideally, in case of an optimal fast sensory system (or a sufficiently soft crash pulse) the crash detection is completed before a significant occupant displacement relative to the vehicle has taken place, since such a displacement reduces the remaining safety space in the vehicle cabin, needed for the *ride-down* with the lowest possible forces. During the crash-detection the seatbelt is unlocked and does not decelerate the occupant - no forces are built up in the seatbelt. The quality of a vehicle sensory system is rated on how fast an incoming crash can be reliably identified after occurrence of the first physical contact, so that a Time-to-Fire (TTF)-signal can be routed to trigger the SBS.

The second in-crash-phase is called *force-closure.* It includes SBS pretensioning and locking, as well as the force build up to the load limiting level initially set. Since the SBS being locked, the relative forward displacement of the ATD is building up the belt forces. In classical passive safety phase 2 is regarded functionally as the most dynamic phase. The functional tasks of slack removal, retractor locking and building up of belt forces is influenced by various factors. The SBS performance depends on the actual in vehicle situation (available belt slack, compressibility of occupant including clothing, belt friction in D-Ring, belt contact to occupant, elasticity in fixation points, etc.) and dynamics (dynamic load on the belt system, vehicle pulse, ...) as well as the subsequent retractor locking, which may be accompanied for example by a more or less pronounced belt force drop, discussed later. Depending on the geometry of the SBS anchor points and the instantaneous ATD kinematics the kinetic belt forces are building-up until the predefined limiting force level is reached, and *force-closure* is completed.

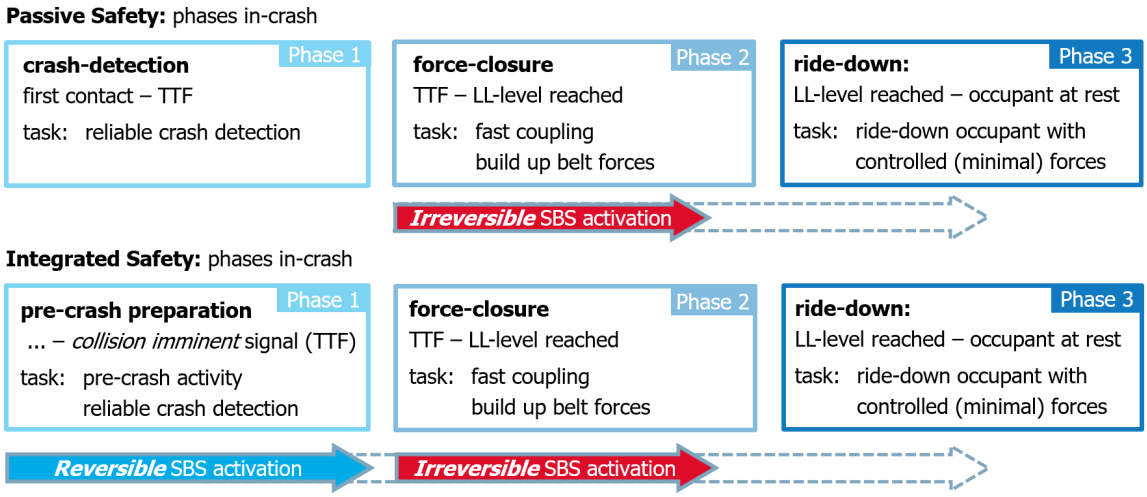

Figure 1 In-crash phases:
first row: The in-crash scenario splits classical passive safety into three distinctive functional segments: Crash-detection, force-closure and ride-down. When assuming a fast crash detection sensory system, only a minor displacement of the occupant relative to the vehicle is expected in phase 1.
second row: Integrated safety pre-crash vehicle maneuvers and reversible SBS activation might move the occupant out of its nominal seating position prior to Time-to-Fire (TTF)-signal, the deployment of irreversible SBS action. Phase 2 starts with initial conditions depending on the pre-crash intervention applied before. Therefore, SBS performance in phases 1 and 2 depend on each other and need to be evaluated together. The ride-down task – phase 3 – utilizing the maximum of the remaining cabin space to ride-down the occupant with minimal forces is identical as in classical passive safety.

The third in-crash-phase describes the *ride-down* of the ATD with controlled minimal forces acting on the dummy through the seatbelt, via friction forces to the seat and to the floor, and if present via airbag systems. During the in-crash phase the relative ATD forward displacement yields in a monotonic, continuous reduction of deceleration distance available in the cabin. The remaining space after *force-closure* shall be completely used to stop the relative motion with controlled forces applied to the ATD, defining the optimum load limiting level for an individual occupant. The handover of the ATD loaded from the belt system into the ATD-airbag contact and the stable capturing of the head is regarded as the major challenge of this phase. Even though the ride-down is a challenging task, it is proportional to the kinetic energy of the ATD entering into the *ride-down* phase and proportional to the available space, hence the combination of both parameter is suggested to measure and to rate the performance of SBS systems.

Integrated safety

As stated by Kramer et al. [14] in chapter 4, within the framework of integrated safety, a clear separation between pre-crash and in-crash phase is no longer possible. One might postulate a “new” starting point for the in-crash phase, as when the vehicle safety electronic control unit (ECU) has decided on an imminent collision. This point in time is either before or after the first physical contact, defined as t=0 s in this paper, depended on the crash prediction / detection algorithm of the SBS ECU. This “new” starting point would exclude reversible, preventive actions, for instance the pre-safe operation of an actively controlled retractor, from the in-crash phase. These types of actuations are triggered by signals interpreted as instable driving situation. If this situation is on top autonomously changed by ADAS intervention it can modify the occupant position via direct forces (example: repositioning of the occupant by belt forces) and / or via indirect forces (inertia forces caused by evasive maneuvers or by emergency braking). Consequently, the initial condition of the occupant in terms of position, velocity, and seatbelt tension forces can become less well defined at the in-crash phase starting point. This will be discussed in more detail on the example of emergency braking. On one hand emergency braking before impact reduces the velocity delta between vehicle and crash target, and thus reduces the crash pulse or even at best avoids the impact altogether, mitigating the safety risk. On the other hand, the occupant’s chest forward displacement caused by braking maneuvers as reported by Mages et al. [15] is likely to reduce the efficiency of SBS pretensioning to remove belt slack, and the *ride-down* could start with an occupant in a less advantageously displaced position. Reversible pre-crash actions can be either assigned to driver assistance or to pre-crash preparation. But all dynamic maneuvers until *force-closure* together represent a continuous transition, which impact the severity of the subsequent force-controlled *ride-down*.

Depicted in the lower row of Figure 1, it is suggested to treat the first relevant deviation in speed between vehicle and occupant as starting sequence for the *crash-preparation* phase. This makes it accessible to physical and virtual testing. A scenario approach combines phase 1 and 2 until the occupant is coupled to the vehicle as *force-closure* is reached. From a functional point of view only the *ride-down,* phase 3 remains unchanged for classical passive and for integrated safety (see Figure 1), thus it can be used to rate on the efficiency of different SBS with the approach suggested in the following section.

HOW TO RATE SEATBELT SYSTEM PERFORMANCE

Component contribution depends upon integral scenario

The performance of a safety system cannot be judged independent from a load case, which is composed of:

1. *Crash scenario:* delta velocity between ego and bullet vehicle, vehicle overlap, impact direction, crash pulse, …
2. *Occupant*: mass, size, feet (fixed to ground or loose), belt routing, …
3. *Vehicle sensory system*: Time-to-Fire delay, ignition strategy for seatbelt & airbags, …
4. *Vehicle*: anchor point geometry, seat adjustment (back rest angle, position), available safety space, crash stability cabin, …
5. *Vehicle seat & environment*: crash-performance seat, pelvis seat immersion (seat stiffness), energy dissipation by seat deformation, friction ATD-seating area, energy dissipation instrument panel, steering column compliance, …
6. *Seat belt system*: retractor-pretensioner (reversible, irreversible, type of pretensioner suitable for load case?), buckle pretensioner, anchor pretensioner, retractor load limiter (constant, switchable, multi-stage, …), buckle load limiter, anchor load limiter, belt webbing, dynamic locking tongue, D-ring (coating), seat integrated SBS, …
7. *Airbag system*: front airbag, knee airbag, seat airbag, airbag in or on belt, …

Therefore, a certain safety target definition is either met or not met by the assessed SBS including ignition and load level switching strategy, i.e., occupant safety is a holistic property of the full load case, and it cannot be attributed to just a single component or sub-system. Although optimal ATD injury risk values are the ultimate goal, it is considered helpful to introduce a metric with a heuristic character. This metric allows to benchmark both – a SBS as well as vehicle attributes like crash pulse severity – separately for each crash phase. It is designed more like the heuristic rating criteria in chess i.e., how to judge on the contribution of a single chess move in an evolved match, to achieve the final goal “checkmate”.

A fast crash detection – as an example – is generally favorable for occupant safety as the TTF-signal, which triggers the irreversible emergency activation, is send out shortly after the first physical contact. This is particularly important in scenarios with hard crash pulses, slow pretensioning systems or small safety spaces. Here the loss of precious safety space of the cabin through unrestricted ATD forward displacement i.e., without decelerating belt forces from a restrained and locked SBS applied is even more important to reach set occupant safety targets. A slower crash sensor may be tolerable in a vehicle with soft pulses and/or large safety spaces.

A more complex question is to rate the efficiency of seatbelt activation (pretensioning, locking, belt force build-up to load limiting level) prior to *force-closure*, reducing partially the kinetic energy of the ATD which coincides with the consumption of safety space, not any longer available in the subsequent *ride-down* of the ATD by controlled forces applied via belt and via airbags systems. The next subsection discusses SBS efficiency prior to the *ride-down* phase and introduces a metric to evaluate it.

SBS efficiency to the point of “force-closure”

When replacing the passenger seat by a generic steel seat with a seating surface inclination of 10° and a backrest position adjusted for the ATD to conserve the initial chest and pelvis position from the analyzed vehicle, the simulation reveals that the ATD crash kinematic in phase 1 and 2 is hardly effected by the seat change (see example of load case LC0 in the appendix A). Consequently, the *force-closure* performance of the SBS can be gauged by means of a generic ideal constant load limiter (CLL) retractor system, which substitutes the original seatbelt system during *ride-down* (phase 3). This transposes the ATD dynamic behavior of the full vehicle setup to a simplified setup where the ATD kinematic can be virtually continued without affecting the natural ATD crash kinematics. The “computed” ideal generic CLL load limiter level required to *riding-down* the energy stored in the ATD at the beginning of phase 3 over a fixed total distance to reach maximum chest forward displacement can be used as metric to quantify the SBS *force-closure* performance.

The procedure is illustrated in Figure 2. The full vehicle configuration has a deformable vehicle seat and a safety system with a switchable load limiter (SLL) and a passenger airbag, which starts to load ATD’s chest and head region at about 55 ms after TTF. Also, at this moment the retractor switches to the lower load level, reducing the occupants shoulder belt force from about 5 kN to 2 kN in order to establish a smooth load onto the ATD during its transition from the seatbelt to the passenger airbag, illustrated in Figure 2 by the black line. The intended first shoulder belt force load limiting level of 5 kN is reached at 40 ms – with *force-closure* being established. When applying the full vehicle system equivalent SBS parameters to the simplified performance measurement setup named “Torso at Seat” (T@S), all relevant dynamic parameters from phase 2 are respected and conserved (green plot Figure 2). To measure the SBS force-closure performance the initial SBS is replaced with the beginning of phase 3 by an ideal generic (CLL) load limiter SBS. All other energy management systems like airbags, switchable load limiters, deformable passenger seats, feet to floor contact friction are taken off, only the non-linear damping characteristics of the deformable passenger seat is modelled on the steal seat by attaching a linear viscous damper to the artificial lower leg to realize comparable generic damping during phase 2. The constant load limiter level in the generic SBS is set in a way, that the chest forward displacement of the ATD stops precisely at 300 mm within ±1.5 mm tolerance. Even though different vehicle configurations do provide more or less safety space to *ride-down* the ATD, the fixed distance allows to better compare SBS configurations in different vehicles.

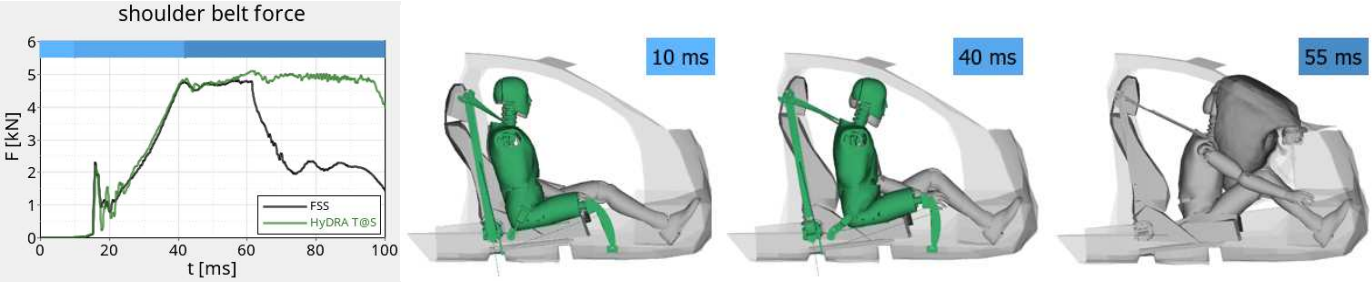

Figure 2 In-crash phases 1-3: Crash-detection, force-closure and ride-down based on shoulder belt force. When using full vehicle system equivalent SBS parameters in the performance measurement setup D.0 (see appendix A), the results from both setups match in terms of shoulder belt force and ATD kinetic for in-crash phases 1-2. For ride-down in phase 3, airbag and load limiting system is replaced by an equivalent CLL system to stop the ATD forward motion at a chest displacement of 300 mm. The simplified T@S-ATD (green) on a steal seat improves repeatability and precision in physical and virtual testing. This load limiting level is used as single value metric to measure the SBS system performance for a given load case.

The ATD preserves its typical kinematic in a vehicle environment, as it depends mainly on the vehicle configuration, which is considered by the metric. Also, the ATD kinematic is not expected to be significantly modified when the ATD interacts with airbags, as these devices are predominantly geared to protect head and neck during late stage of the ride-down phase and to decelerate the ATD by applying pressure over a larger ATD contact area than the belt. Therefore, the occurred kinetic energy reduction of the ATD is well described by its effect on chest forward displacement. When defining the total chest forward displacement for the ATD to come to a halt after ride down at 300 mm the theoretically required CLL level of the generic seatbelt system can be computed. This derived CLL level is called *characteristic shoulder force level* (CFL) and is used as single value metric: A lower absolute CLL level indicates a better SBS performance prior to *force-closure*. Cause and effects relative to a reference system become easily accessible by simple force level comparison.

Fortunately, by means of this metric, the parameters of the vehicle configuration can be transferred onto a simplified set-up with *reusable* rigid seat with *stable* dynamic system characteristic, yielding in more efficient testing as well as more efficient simulation. The transfer from a validated full vehicle system model to the simplified setup, as well as sensitivity studies on geometrical parameters with the simplified setup, are shown and discussed in detail in the appendix A. From there it can be derived that it is adequate to characterize any vehicle configuration in the simplified setup by *eight* adjustable quantities.

Simplified generic load case described by “The BIG 8”

To summarize the findings from the example configurations in the appendix A, the load case is fully characterized by the following eight parameters, and the *force-closure*-performance can be assessed appropriately with simplified setups like D.0:

1. *Vehicle pulse:* SBS fixation point deceleration time sequence in for-aft direction
2. *Time-to-fire delay:* earliest point in time an imminent crash is safely detected
3. *ATD:* mass & stiffness distribution, kinematics, feet sliding / footrest, ...
4. *Initial Torso inclination:* H-angle dependent on backrest orientation
5. *SBS fixation points:* D-ring, buckle, and anchor relative to seat
6. *Pelvis damper force:* deceleration through seat friction in phase 2, restraining forces due to deformation, and geometric interlock in phase 3, defined in the simplified T@S-setup by a damper characteristic to provide damping of a generic seat
7. *System slack:* webbing on spool, configuration slack (chest & pelvis), buckle head movement, chest compression, …
8. *Available safety space:* max chest forward displacement without body to interior impact

These parameter-set is designated “The BIG 8”. Assuming vehicle specific recommended values for item 2-8, item 1 - *vehicle pulse* heavily depends on the load case vulgo crash scenario. This list of items could be extended where appropriate by two robustness parameters.

I. *Part temperature*
II. *New / aged parts*

Using an identical SBS (3-PGA) and an identical control strategy in different vehicle configurations defined by “The BIG 8” it is possible to compare these configurations by the metric introduced in Figure 2, to be discussed in the next section.

Vehicle load case benchmark and quantification

“The BIG 8” characterize a vehicle configuration, and by applying an identical SBS mounted in different vehicle configurations the single value metric “CLL level maximum 300 mm chest forward displacement” allows to compare and eventually to rate different vehicle load cases. The resultant CLL level is referred to as *characteristic shoulder belt force* level (CFL). This is done exemplarily for the configurations from Figure 14 and from Figure 17 i.e., under load case CL0 without pre-braking. The absolute

(CFL), the delta (dCFL) and relative (rCFL) characteristic shoulder belt force levels are printed in

Table 1. The first row shows the absolute force level, and the second row the difference between the individual configuration and the *Pretty Good Vehicle* (PGV) - configuration (D.0), the chosen reference vehicle as delta (in N) and as percentage, calculated according to

$$dCFL_{D.x} \coloneqq CFL_{D.x} - CFL_{D.0} \quad ; \quad rCFL_{D.x} \coloneqq \frac{CFL_{D.x} - CFL_{D.0}}{CFL_{D.0}} \;, for\ x = 1,2,3,4. \tag{1}$$

Table 1

Characteristic shoulder force levels (CFL) for configurations of Figure 17 using SBS-1 and SBS-2 when subjected to LC0 - no braking load case. Relative CFL for SBS-2 and SBS-1 show about same percentage.

	Vehicle Configuration			D.0	D.1	D.2	D.3	D.4
Seatbelt System SBS	LC0 T@S			HyDRA T@S baseline	anchor slack +40 mm	backrest +5°	anchor & buckle fixation - 100mm	D-ring -200mm
SBS-1	absolut characteristic shoulder force level	CFL_D.x	in N	10000	10600	8600	6200	7400
	relative characteristic shoulder force level	dCFL_D.x	in N	0	600	-1400	-3800	-2600
		rCFL_D.x	in %	0,0%	6,0%	-14,0%	-38,0%	-26,0%
SBS-2	absolut characteristic shoulder force level	CFL_D.x	in N	8800		7700		6400
	relative characteristic shoulder force level	dCFL_D.x	in N	0		-1100		-2400
		rCFL_D.x	in %	0,0%		-12,5%		-27,3%

The results indicate that the SBS shows significant differences between configurations. Configuration D.3 is most advantageous followed by D.4 and D.2. The added slack at the anchor in Configuration D.1 leads to a rating inferior to that of D.0 (PGV), which is consistent to the fact, that the pretensioner is not able to remove all slack added at the other end of the belt. These results displayed graphically in Figure 3 confirm well the conclusions derived from the detailed analysis in appendix A. The SBS with a different pretensioner type, SBS-2, subsequently used as reference seatbelt system *Pretty Good Seatbelt System* (PGS) was evaluated for vehicle configuration D.0, D.2 and D.4. The absolute CFL levels for vehicle configuration D.0 differ between SBS-1 and SBS-2 but the relative characteristic forces from Figure 3 show the same trend for both SBSs, allowing the classification of vehicle configurations.

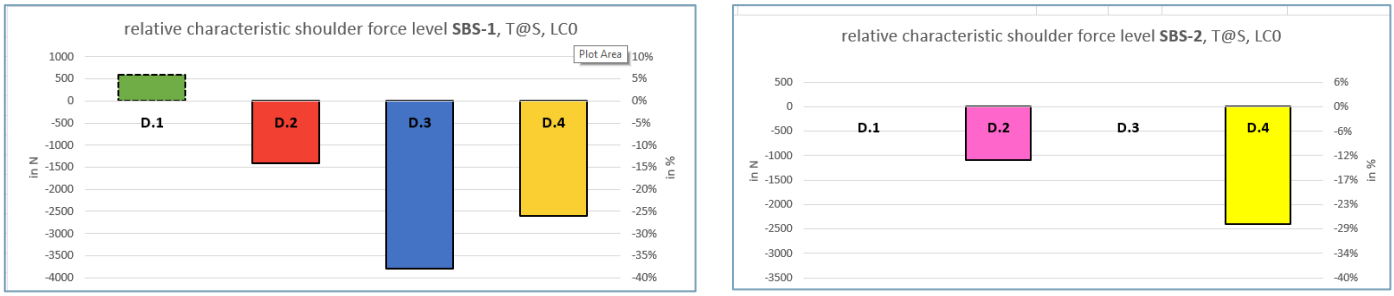

Figure 3 Vehicle configurations D.1-D.4 relative to D.0 compared by relative characteristic shoulder force (see Table 1) for seat belt system SBS-1 (left picture) and for SBS-2 (right picture D.0, D.2, D.4) with ATD T@S under load case scenario LC0

This investigation is an example of how different vehicle configurations (defined by "The BIG 8" parameter set) can be compared with this metric, simply by using an identical SBS (3-PGA system and activation strategy). Alternatively, this approach can be used to rate different SBS systems or/and different SBS control strategies in each target vehicle configuration, which will be discussed in detail in the following section.

SBS PERFORMACE BENCHMARKING

In this section three different SBS systems with their individual control strategies are mounted and assessed in the PGV geometry and three different vehicle load cases are applied: Load case LC0 consists of the US NCAP pulse for the PGV, whereas load case LC1 and LC2 incorporate the effect of two different pre-braking load cases, as illustrated in Figure 4.

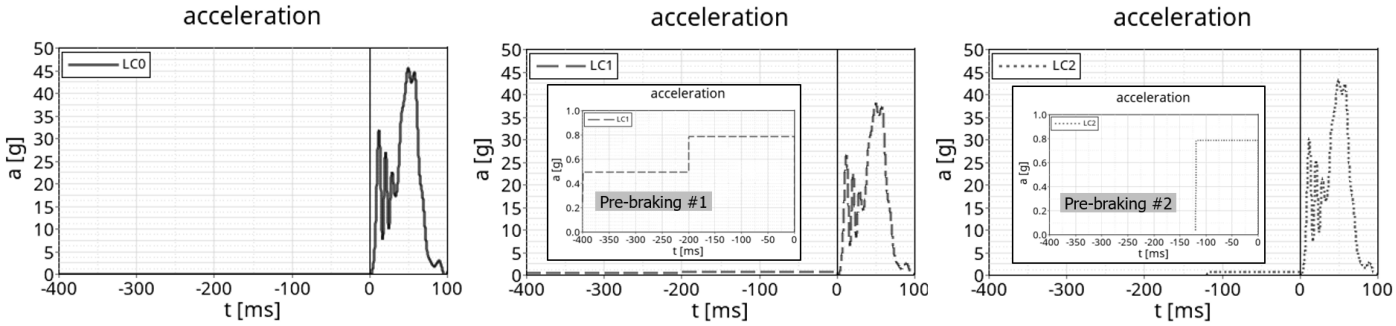

Figure 4 ***Left picture - LC0: US NCAP pulse of the PGV for FWFI at 56 km/h.***
Center picture – LC1: Long pre-brake pulse, starting at 400 ms before the crash with plateaus of 0.5 g and 0.8 g, each lasting for 200 ms, followed by actual crash pulse. Pre-braking reduces the impact velocity by 2.6 m/s, accounted for by applying a factor of* 0.833 *to the pulse.
Right picture – LC2: Short pre-brake action starting at 120 ms before the crash, with a plateau of 0.8 g lasting for 120 ms, followed by the US NCAP pulse multiplied by a factor of 0.94.

Since t=0 s is defined as physical start of the crash i.e., time of first vehicle to obstacle contact, pre-crash activation shows a negative timestamp. The first pre-braking load case LC1 - consists of stepping up from 0.5 g level to 0.8 g level, with each level being maintained for 200 ms, which slows down the velocity of the target vehicle by 2.6 m/s. This is accounted for by applying a factor of 0.883 (see equation (2)) to the pulse. The second pre-braking load case LC2 consists in immediate maximum braking with 0.8 g for 120 ms prior to the crash, with the original crash pulse scaled by a factor of 0.94. Here-in it is assumed that the reduced delta velocity between barrier and target vehicle can be accounted for by simply downscaling the US NCAP pulse of the PGV for FWFI subsequent crash pulse by a factor of

$$\frac{v_0-\Delta v_{braking\_\#1}}{v_0}=\frac{15.56-2.6}{15.56}=0.833 \quad \text{and} \quad \frac{v_0-\Delta v_{braking\_\#2}}{v_0}=\frac{15.56-0.96}{15.56}=0.94 \quad . \qquad (2)$$

The following three different SBS systems were selected for this investigation:

SBS-1: Pretensioning via spool-coupling, CLL 3 kN, TTF 10 ms, Standard D-Ring, Standard buckle

SBS-2: *Pretty Good Seatbelt System* PGS: Pretensioning via torsion-bar-coupling, CLL 3 kN, TTF 10 ms, Standard D-Ring, Standard buckle

SBS-3: Actively Controlled Retractor ACR, CLL 3 kN, TTF 10 ms, Standard D-ring, Standard buckle with two different start *reversible pull-in activation* (RPA) times:
RPA1: Activation at $t = -400\ ms$
RPA2: Activation at $t = -120\ ms$

The dynamic ATD response is described by time sequences of three force / displacement pairs: Recording quantities are, at the retractor; retractor force / webbing pay-out, at the upper body; shoulder belt force / chest forward displacement, and at the lower body; anchor belt force / tongue slip. Figure 5 to Figure 7 display the results gathered for the load cases LC0, LC1, and LC2.

The design of the two retractor pretensioners, SBS-1 and SBS-2, differ significantly in their torque loading path from the pretensioning unit into the spool. Regardless of this fundamental difference, it has barely an impact on pretensioner force peak levels and on pretensioning pull-in speeds, but it yields in a different locking behavior, resulting in different slopes to finalize the *force-closure*. In comparison to SBS-1, SBS-2 pulls-in a significantly larger amount of webbing and the force drop accompanying the inversion of the spool rotation being less pronounced. SBS-2 reaches the CLL level slightly earlier than SBS-1. Other than expected from their close chest forward displacement curves in Figure 5, all these advantages of the SBS-2 do lead to a significant change in the characteristic shoulder force levels (CFL) in Table 2 which differ by 1200 N between SBS-1 and SBS-2 i.e., 13.6%. The absolute CFL values are related to the energy (work) of the shoulder belt force and to the displacement remaining after *force-closure* as discussed in appendix B.

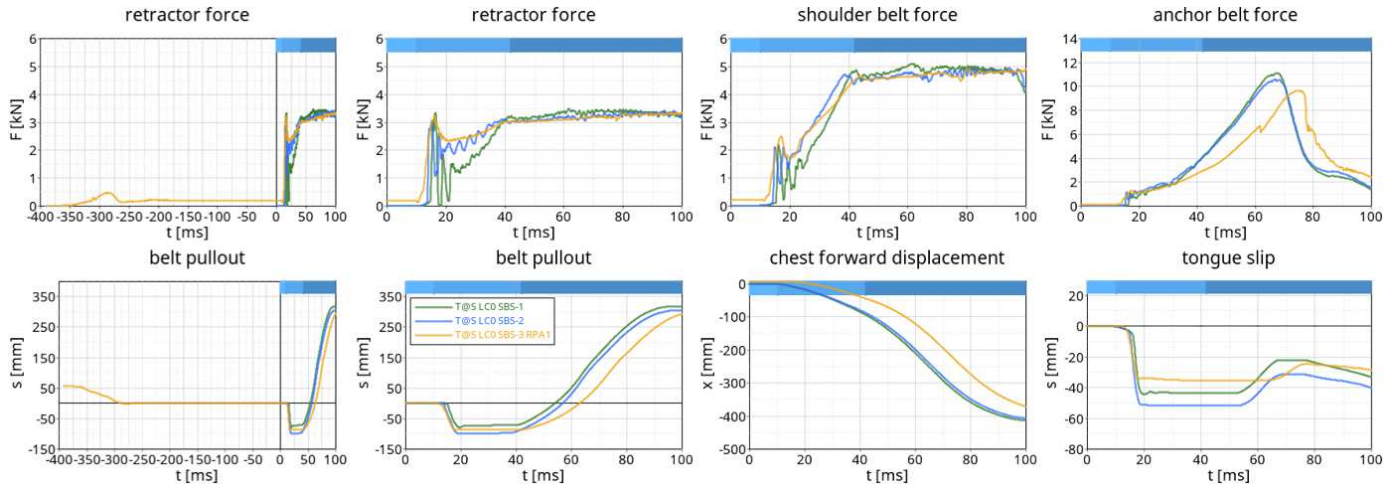

Figure 5 Dynamic T@S-ATD response when subjected to LC0 (US NCAP pulse of the PGV for FWFI at 56 km/h as shown in Figure 4 (left picture)) for three SBS configurations. Standard pretensioners SBS-1 and SBS-2 differ in the transition to force-closure, apparent on the force readings at the retractor and at the shoulder. Their small difference in chest forward over 400 mm displacement constitutes a considerable difference in CFL of 1200 N. SBS-3 with early activation (RPA1) causes the chest forward displacement to be reduced by 79 mm at t=60 ms, advantageous to unfold a frontal airbag. CFL refer to Table 2.

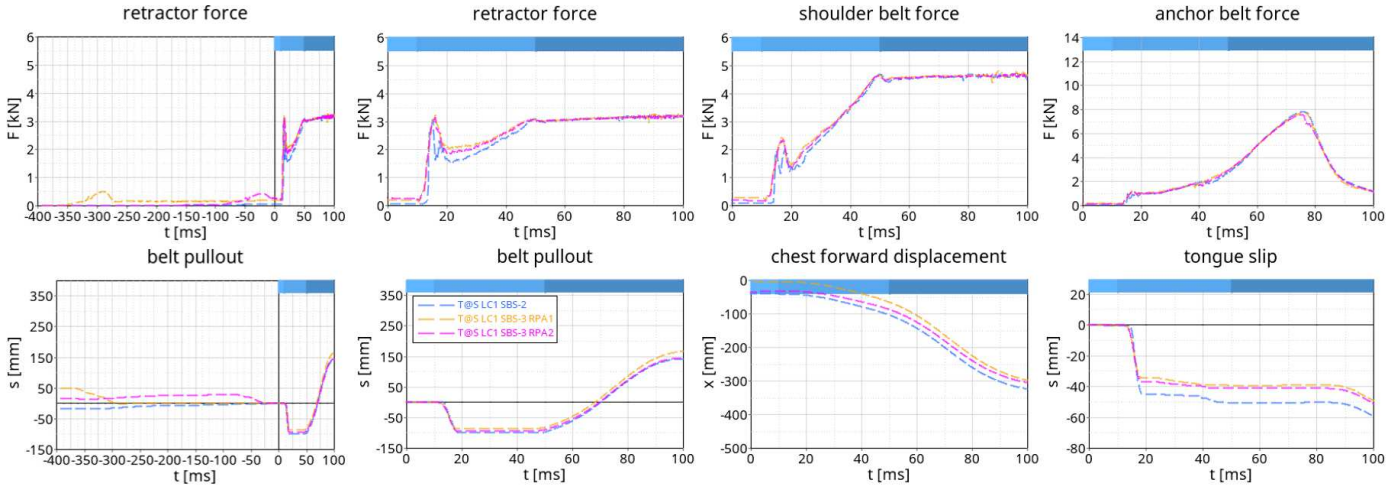

Figure 6 Dynamic T@S-ATD response for LC1 for three different SBS configurations. Early SBS-3 activation with RPA1 is of advantage compared to RPA2, chest forward displacement at t=60 ms is reduced by 38 mm, and by 18 mm respectively to standard non-active pretensioner SBS-2. Corresponding CFL refer to Table 2.

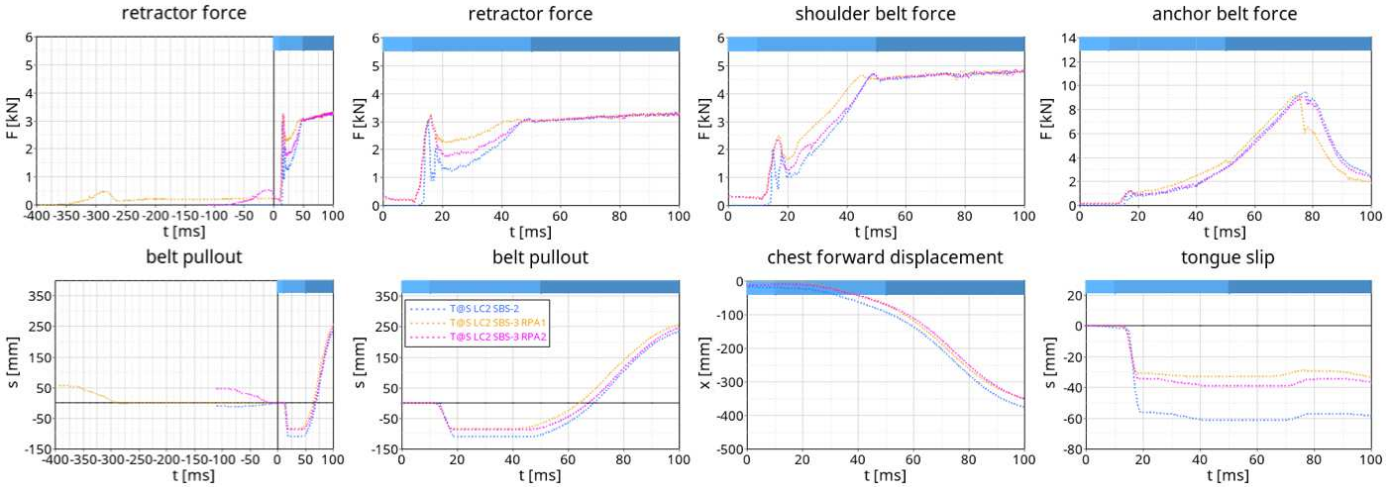

Figure 7 Dynamic T@S-ATD response for LC2 for three different SBS configurations. Simultaneous pre-braking and activation of SBS-3 (RPA2) results in similar CFL rating compared to early ACR activation (RPA1). Both ACR activation strategies show a similar benefit, the chest forward displacement at t=60 ms is reduced by 18 mm and 26 mm compared to a traditional pretensioner system. Corresponding CFL refer to Table 2.

However, the actively controlled retractor (ACR, SBS-3) shows, due to the early intervention, a consistent improvement for all load cases. In the pre-braking scenario, LC1 displayed in Figure 6, the effect of the active intervention is as expected more pronounced than for LC2 shown in Figure 7, as the braking induced ATD chest forward displacement in LC1 has more time to evolve for standard pretensioners i.e., without active intervention. With the conventional pretensioner SBS-2 the chest shows already a forward displacement of 40 mm (LC1) respectively 17 mm (LC2) prior to the crash. The RPA1 pre-activation from SBS-3 generates a shoulder belt force of about 200 N in the pre-braking scenario, which is apparently strong enough to prevent ATD forward displacement under braking deceleration for all load cases LC0-LC2. Late activating of SBS-3 (RPA2) in load case LC1 with early braking (see pink line in Figure 6) results in a chest forward displacement prior to crash of 34 mm. The reversible pre-crash activation, latest simultaneously with the pre-braking operation, of SBS-3 reduces significant slack by aligning the belt system at moderate forces before the crash. The belt pull-out is set to zero at t=0 s, start of the actual crash pulse to ease the comparison of pretensioning and crash dynamics for different systems. Consequently, for ADAS activation, before t=0 s, pre-crash webbing pull-in shows up above and pre-crash belt pull-out shows up below the neutral axis. Although the pretensioning of SBS-3 works on an already slack reduced seat belt system, the SBS-3 is able to pull-in almost the same amount of belt as SBS-2, with both systems using an identical pretensioning mechanism. The higher retractor force level between pretensioning and *force-closure* for SBS-3, results from lower belt system slack due to the pre-crash belt slack removal. The shallower slope to *force-closure* of the shoulder belt force from SBS-3 correlates with a slower ATD chest forward displacement, indicating that the impulse passed from the 200 N pre-tensioning force onto the ATD upper body is high enough to retard the chest forward displacement. At t=60 ms the difference in chest forward displacement between SBS-2 and SBS-3 amounts to 79 mm for LC0, 38 mm for LC1 and 18 mm for LC2, not only in a lower total chest forward displacement, but more importantly the *retarded* chest forward displacement allows a frontal airbag system to safely unfold in front of the ATD chest.

Also of advantage, the early slack reduction with low forces modifies the anchor belt force vs. time characteristics visible in Figure 5 when comparing SBS-1 and SBS-2 to SBS-3. Figure 6 and Figure 7 reveal that the advantageous anchor belt force behavior is conserved as well for LC1 and for LC2. The slow pre-crash belt slack removal, even by pre-braking without ACR activation transduces into the pelvis region. This is not equally accomplished by the irreversible highly dynamic retractor pretensioning operation. The analysis suggests that a contact with beneficial significant friction forces between seat area and ATD is realized by the pre-crash slack removal.

On one hand, pre-braking reduces the vehicle velocity before the impact, i.e., the crash pulse becomes softer and softer, the longer the braking interval lasts - being in general of advantage to improve occupant safety. On the other hand, the chest forward displacement at *force-closure* is prone to be larger with pre-braking than without pre-braking, yielding in a reduction of safety space for the ride-down phase.

Whether an AEB intervention is likely to mitigate a crash event does not only depend on the length of the braking interval and the availability of an actively controlled safety system, but it also depends on the level of the braking deceleration in combination with the individual occupant reaction - to be discussed in the following section.

PRE-CRASH ANALYSIS UNDER LOW G

Limited suitability of ATD for low g pre-crash analysis

Traditional crash ATDs are not suited to predict occupant reaction for decelerations below 1 g. Mages et al. [15] compared experimentally the chest displacement of an H350 ATD with the chest displacement of human test persons during physical drive tests, whereas Schilling et al. [19] approached this subject by simulating virtual load cases comparing the response of an active SAFER-HBM with the response of H350- and THOR-ATD models. Both publications conclude that there is a significant difference in the chest forward displacement at low g levels between the human body and the ATDs. The ATDs tend to show significant lower upper body displacements compared to human occupants, being related to a stiff non-biofidelic pelvis region.

Recent preliminary braking tests on tarmac and on gravel were performed with a compact class vehicle to simulate the behavior of a sleeping front passenger on the basis of three different occupants only (including the authors). When subjected to deceleration levels below 0.5 g occupants react individually, depending on the individuum and its alertness, being warned or unwarned of the impending braking, either the upper body will be thrust into the locked seatbelt, or the upper body will be stabilized by tightening pelvis muscles. When being in a relaxed initial status, without consciously tightening the pelvis muscles, dynamic chest forward displacement into the locked seatbelt is assumed to occur for vehicle decelerations exceeding 0.75 g. The impressions gained from these first-off braking tests can be summarized to: once the dynamic chest forward displacement is initiated the motion is more governed by the inertia distribution of the human occupant, muscle activities do not play a major role any longer. To simulate this effect, a simplified generic ATD geometry was developed and machined to be discussed in the upcoming section.

Simplified ATD with instant response time

The simplified generic ATD substitute named “Rebound Guy Mk I” (RBGI), with two major Degrees of Freedom (DOF) only, as depicted in Figure 8, is designed to generate for impacting crash pulses a kinematic response that compares to the H350-ATD shown on the right picture of Figure 8. The moment of inertia of the upper body relative to the swivel-joint, connecting upper to lower body as well as the position of the lower body itself are the key parameters for this kinematic. The basic configuration with H350-ATD like moment of inertia can be easily changed with lump masses either by adding to or by removing from the upper

body. Slack is accounted for by two elements one in the chest and one in the pelvis region, and the amount of slack is adjustable. The initial inclination of the upper body can be varied from 0° - 45° to the vertical. Bump stops visible in Figure 8 limit the back-and-forth rotation of the upper body and the linear transition of the lower body. Loading SBSs with this simplified RBGI geometry increases test efficiency, accuracy, and repeatability.

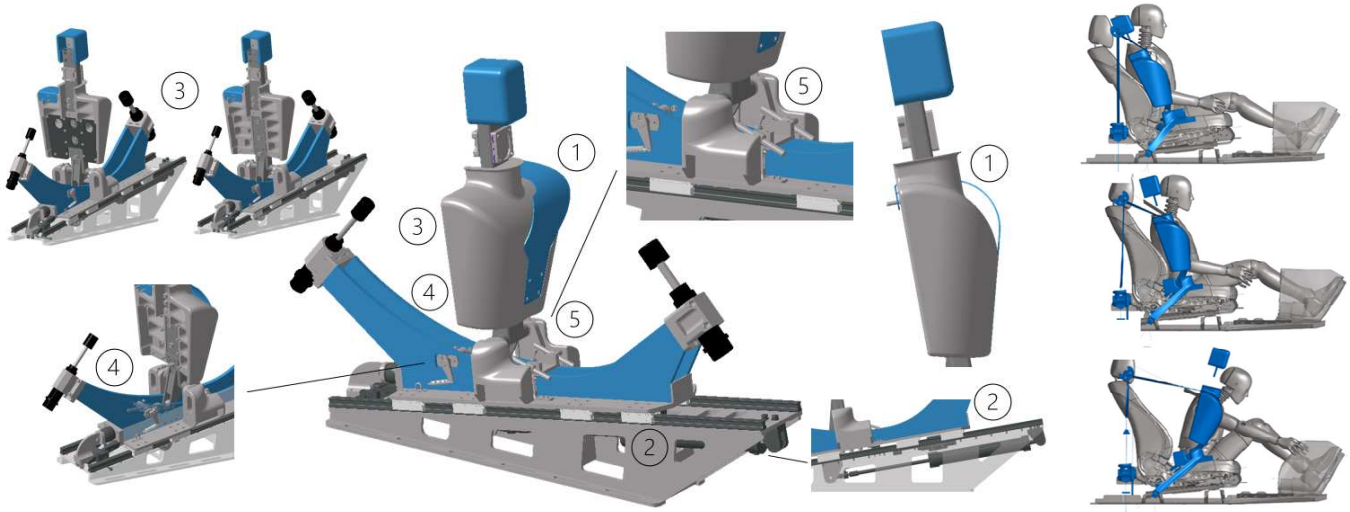

Figure 8 ***CAD (left picture) and kinematic (right-hand picture) of generic ATD "Rebound Guy Mk I" (RBGI) with two major DOF: DOF 1, upper body connected via swivel-joint to lower body; DOF 2, lower body railed on ball bearings sliding up a 10° slope. Bump stops limit the chest rotation and the pelvis displacement. Features: ① chest slack, ② lower body viscous damper, ③ variable moment of inertia adjustable by trim masses, ④ adjustable initial upper body inclination, ⑤ pelvis slack. The RBGI is placed inside a frame to attach the seatbelt system, which represents the PGV configuration. Recording damper force, lower body displacement and upper body rotation angle provides accurate monitoring of the RBGI kinematic useful for Digital Twin validation. Right-hand picture: Comparison of RBGI kinematic relative to H350 ATD subjected to LC0.***

The reduced DOF allows a faster and more accurate initial ATD positioning. Altogether the setup guarantees a more stable and repeatable system behavior (no fatigue of rubber components, defined slack, etc.) and the kinematics is precisely monitored by an integrated sensing system (damper force, lower body displacement, upper body rotation angle). This build-in motion monitoring system allows a direct forward-backward transfer of kinematic results between the physical and the virtual world, offering a major benefit to identification and validation work. With regards to pre-crash activation at low g-levels the undamped, inertia dominated rotation of the upper body causes an instant response, considered to be closer to the reaction of an unwarned occupant not tightening the pelvis muscles, than to the response of the H350-ATD. The stiffness of the RBGI slack elements under SBS pre-crash activation can be further improved to better correspond to a H350-ATD slack resistance.

The simulation results with RBGI-ATD subjected to LC1 are displayed in Figure 9 and Figure 10 shows the results for LC2 accordingly. The results are displayed in the way as the results gathered with the T@S-ATD (Figure 6 and Figure 7) allowing a directly response comparison between the different ATDs for identical load cases. At crash contact (t=0 s) for LC1, without ACR pre-crash activation whilst braking, the RBGI-ATD chest forward displacement reaches 100 mm compared to 40 mm only for the T@S-ATD. This is illustrated in Figure 11 via a side view of the ATDs, T@S (green) and RBGI (red) and SBS-2 subjected to LC1 for the time stamps: t=-0.4 s, t=-0.2 s and t=0 s. An early ACR activation like RPA1, starting with the pre-brake maneuver, can prevent chest forward displacement in the pre-crash phase for both ATDs. The advantage of the ACR (SBS-3, RPA1) is more pronounced for the agile ATD RBGI showing 100 mm less chest forward displacement at t=60 ms than the standard SBS-2 pretensioner (see Figure 9) whereas the difference when using the T@S-ATD reaches only 40 mm (see Figure 6). Reduced chest forward displacement at t=60 ms is beneficial as the frontal airbag can unfold more freely.

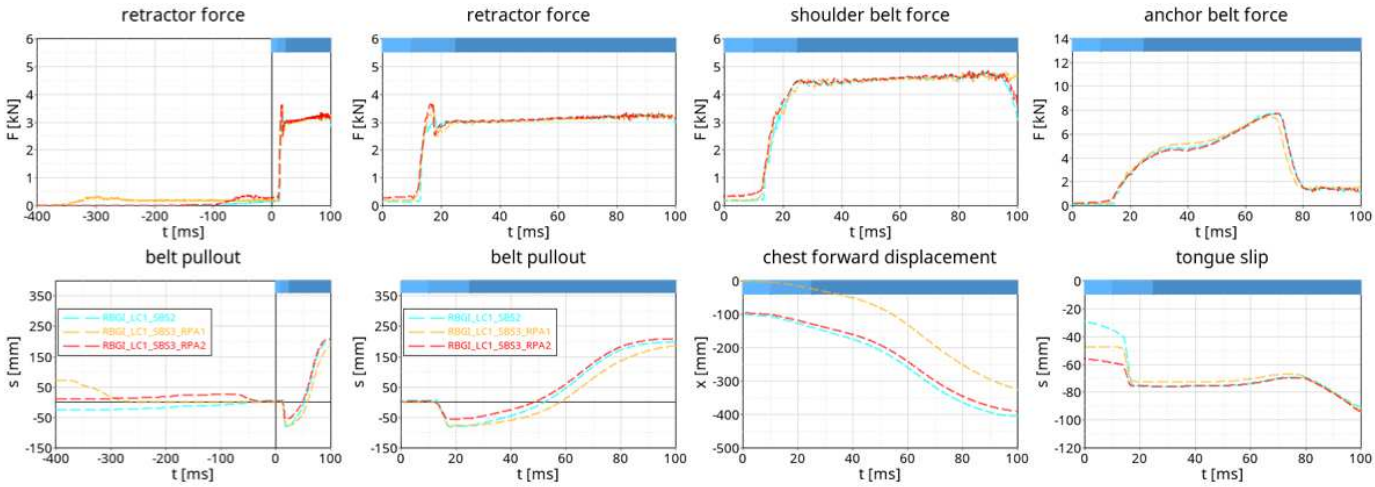

Figure 9 Dynamic response of RBGI subjected to load case LC1 with long pre-braking pulse described in Figure 4 (center picture) for SBS-2 and SBS-3. Comparison with Figure 6 illustrates, that RBGI-ATD shows a higher sensibility to braking action than T@S ATD, suggesting that RBGI-ATD can be regarded as a worst-case scenario representing a sleeping hence relaxed occupant. Pronounced differences in anchor force readings for RBGI-ATD and for T@S ATD will be addressed by further optimization work on the lower body.

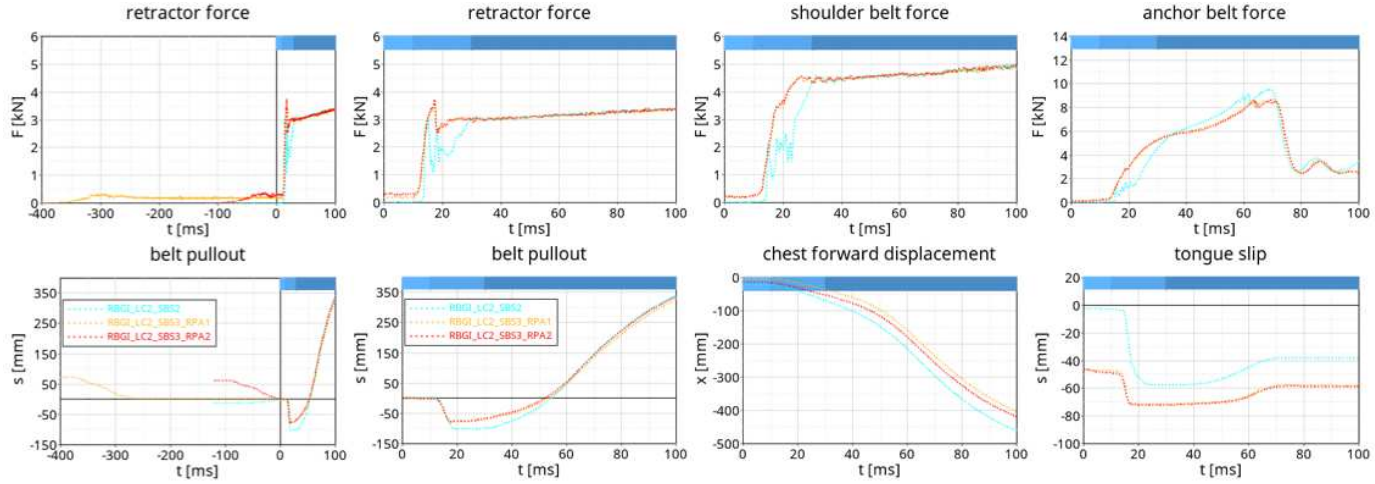

Figure 10 Dynamic response of RBGI subjected to load case LC2 with short pre-braking pulse described in Figure 4 (right picture) for SBS-2 and SBS-3. Comparison with Figure 7 illustrates, that RBGI-ATD shows a higher sensibility to braking action than T@S ATD. Differences in anchor force readings for RBGI-ATD and for T@S ATD analogous to LC1.

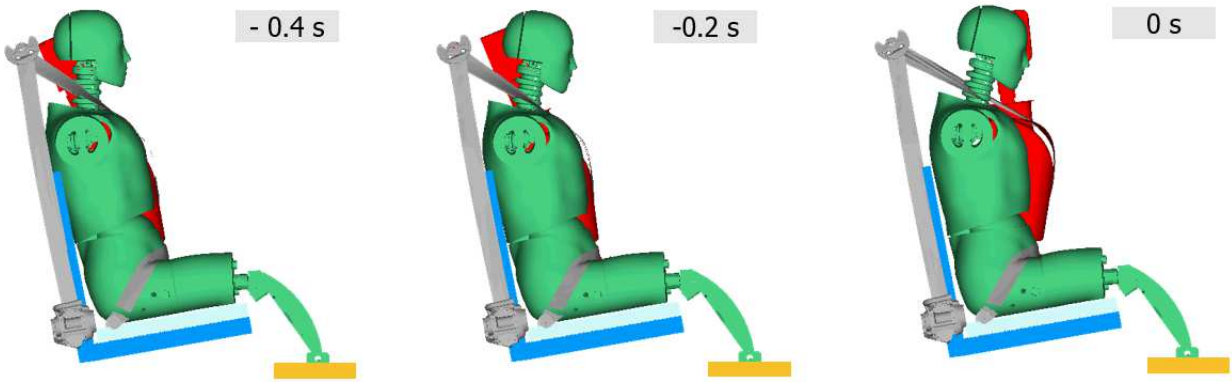

Figure 11 RBGI-ATD (red) compared to T@S-ATD (green) for LC1 initial (left picture), subjected to 0.5 g deceleration (middle picture), and subjected to 0.8 g deceleration (right picture). RBGI more sensitive to low g activation due to higher mobility at upper hip when deceleration level exceeds 0.5 g.

Table 2

Characteristic shoulder force levels for different SBS systems in PGV vehicle configuration with two different occupants: T@S-ATG and RBGI-ATG subjected to crash pulse LC0, LC1 and LC2 (as illustrated in Figure 4). The difference between T@S and RBGI response are best observed under LC1, with extended braking time. RBGI chest forward displacement response for low g acceleration might be considered as worst-case scenario for human occupants.

	Seatbelt System SBS		SBS-1	SBS-2 = **PGS**	SBS-3	SBS-3
Vehicle Configiguration	T@S D.0 = **PGV**		TTF+10ms	TTF+10ms	RPA1 & TTF+10ms	RPA2 & TTF+10ms
T@S D.0 LC0	characteristic shoulder force level	in N	10000	**8800**	7100	
	relative characteristic shoulder force level	in N	1200	0	-1700	
		in %	13,6%	0,0%	-19,3%	
T@S D.0 LC1	characteristic shoulder force level	in N		**5400**	4800	4800
	relative characteristic shoulder force level	in N		0	-600	-600
		in %		0,0%	-12,5%	-12,5%
T@S D.0 LC2	characteristic shoulder force level	in N		**7800**	6300	6600
	relative characteristic shoulder force level	in N		0	-1500	-1200
		in %		0,0%	-19,2%	-15,4%
RBGI D.0 LC0	characteristic shoulder force level	in N		**10650**	8000	8000
	relative characteristic shoulder force level	in N		0	-2650	-2650
		in %		0,0%	-24,9%	-24,9%
RBGI D.0 LC1	characteristic shoulder force level	in N		**7400**	5200	6350
	relative characteristic shoulder force level	in N		0	-2200	-1050
		in %		0,0%	-29,7%	-14,2%
RBGI D.0 LC2	characteristic shoulder force level	in N		**10150**	6900	7350
	relative characteristic shoulder force level	in N		0	-3250	-2800
		in %		0,0%	-32,0%	-27,6%

Since the RBGI kinematic is more sensitive to inertia effects Table 2 reveals a significant difference between the results obtained with RBGI and the results obtained with T@S. The results with RBGI-ATD highlight even more the benefit of early reversible-restraint activation (LC1 30 % improvement compared to 13 %, LC2 32 % improvement compared to 20 %). The design intended removed stiffness in the RBGI's "pelvis region" causes with braking a direct chest forward displacement (being inertia related it needs time to build up) relative to the fixation points, and the associated belt pull-out takes place without generating significant belt forces. This chest forward displacement represents a loss in safety space and it cannot be recovered i.e., by pretensioning, once lost. This explains why the seatbelt system without active pre-safe option yields an inferior performance with RBGI than with T@S-ATD: With active controlled retractors (ACR) and an early pre-safe activation, ideally before pre-braking, the initial safety space can be conserved before the actual crash occurs.

Rating various contributions to occupant protection

A comparison of the absolute characteristic shoulder force levels between load case LC0 (impact without pre-braking), LC1 (long pre-braking) and LC2 (short emergency pre-braking) in Table 2 for T@S-ATD and equally for RBHI-ATD reveals, that pre-braking – the longer the better – is beneficial for occupant safety independent of the seatbelt system. This is especially remarkable for LC2. Even in the case where the impact occurs shortly after the emergency braking is initiated, the loss in safety space by an unrestricted chest forward displacement accompanying the braking deceleration is still sufficiently compensated by a softened pulse due to the reduced impact velocity.

Following the strategy to use the *Pretty Good Vehicle* (PGV) configuration and *Pretty Good Seatbelt-System* (PGS) as references allows to compare even the effect of different dimensions from "The Big 8" on occupant safety. I.e., the results from Table 2 permit to conclude, that the safety improvement with an active controlled retractor (T@S D.0 LC0 SBS-3 RA1: CFL=7100 N) relative to the reference (T@S D.0 LC0 SBS-2: CFL=8800 *N*) is somehow comparable to the improvement by pre-crash braking. The ACR result is bracketed by the results gathered with the PGS for long (T@S D.0 LC1 SBS-2: CFL=5400 N) and for short emergency braking (T@S D.0 LC2 SBS-2: CFL=7800 N) maneuvers. An effect in the same order of magnitude can be achieved by changing the vehicle configuration. The ACR benefit can be rated, according to Table 1, between a 5° steeper backrest (T@S D.2 LC0 SBS-2: CFL=7700 N) and D-ring fixation point moved by 200 mm to the rear (T@S D.4 LC0 SBS-2: CFL=6400 N), provided that the result is not biased by a changed ratio of chest to shoulder belt displacement as discussed in appendix B.

In principle each of the "The Big 8"-parameters can be optimized using the proposed CFL-metric. Crash-pulses for example can be rated to optimize the crashworthiness of vehicle structures by comparing the CFL measured in PGV configuration with PGS restraint system for different crash pulses. This way a much more specific rating is obtained, than by applying some of the crash pulse criteria discussed by Kuebler et al. [16], which are derived either directly from the pulse by means of simple mathematical operations or based on simplified mechanical models e.g., Occupant Load Criterion (OLC).

From the validated reference simulation model based on PGV and PGS the rating based on CFL are readily obtained and can be verified by testing as to be discussed in the next section.

HARDWARE TO TEST SBS PERFORMANCE ON SLED FOR SIMULATION ANCHORAGE

The simplified generic ATD substitute also referred to as “Rebound Guy Mk I” (RBGI) depicted in Figure 9 is built in hardware to be run on a test bench called “Hyper Dynamic Response Actuator”, shown in Figure 12 (photo left), and presented in detail by Machens et al. [10]. The test bench consists of a rail guided carbon sled driven by nine closed loop controlled electric linear motors running along a 6-meter track. Active control of sled acceleration and deceleration opens the field of experimentally analyzing effect of pre-crash and in-crash dynamics - incorporation of ADAS operation and ACR activation during the test sequence.

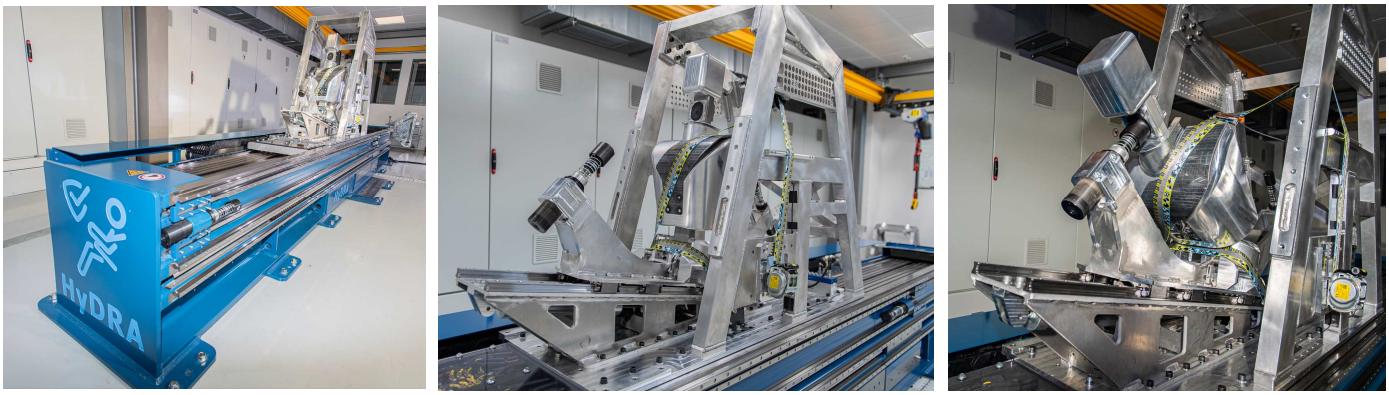

Figure 12 “Rebound Guy Mk I” (RBGI) on HyDRA® (see [10]) test bench (photo left). Close up before the test (photo center) and after the test (photo right). The SBS is fitted on a lightweight aluminum frame structure, designed to represent the PGV vehicle coordinates but it allows also to vary fixation points. Viscous damper with force load cell hidden underneath lower body rail.

The seatbelt system is connected to a lightweight frame structure out of aluminum, which is mounted onto the carbon sled. Although standardized testing with the generic PGV configuration is recommended to assess SBS performance, SBS fixation points can be varied within a certain range. With a maximal propulsion power of 120 kN on HyDRA® test bench a typical RBGI setup can be accelerated up to 30 g. This allows to combine dynamical effects from pre-crash ADAS activation, typically below 1 g acceleration, to be followed by a significant crash-pulse, allowing to assess and to optimize SBS functionalities on these important real-world safety load cases. To simulate different backseat inclinations the initial angle of the RGBI’s upper body can be set between 0-45° degree to the vertical (Figure 8).

A second simplified test-bench setup called Torso@Seat (T@S) consists of an adapted H350-ATD as illustrated in Figure 13. This setup serves to link bench results to actual standardized crash test results and is particularly versatile, when reproducing test results from a full-scale vehicle crash or from a sled test configuration with H350-ATD to analyze and optimize effects on the HyDRA® bench. This simplified bench test setup, already used as a simulation model in Figure 3 consists of a H350-ATD with the under legs replaced by a hinged stiff gear, connected to a viscous damper. The H350 arms are replaced by lumped masses with different weights fitted to the shoulder hinges. In this configuration the backrest of the rigid seat can be adjusted between 0°-45°

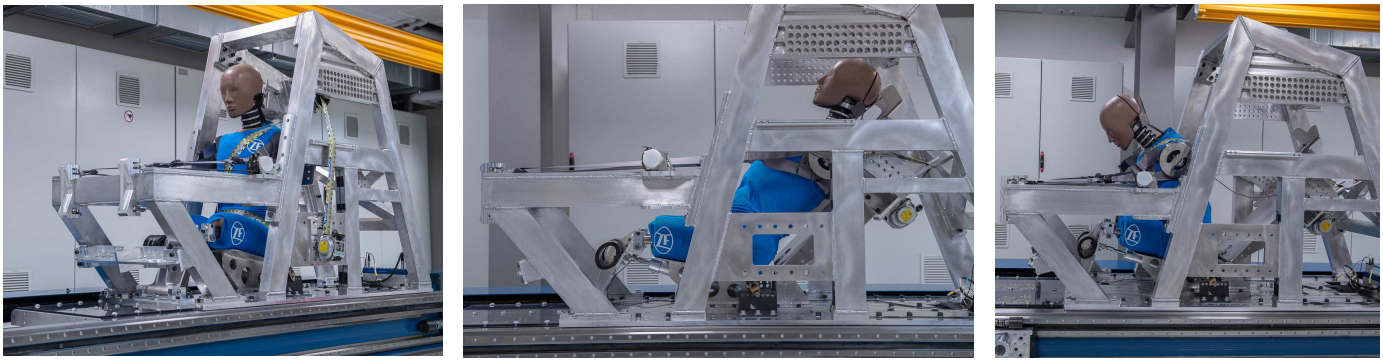

Figure 13 HyDRA® H350 Torso@Seat (T@S) setup before test with 10° (left picture) and with 45° (center picture) back rest angle and after test (right picture). The ATD is trapped in the forward position by a SBS with a pair of retractors especially designed for fast belt pull-in. ATD is placed inside a lightweight aluminium farme structure with PGV SBS coordinates. Setup details: hinged stiff gear substituting the under leg, adaptive viscous damper, bump stops, arm mass substitutes, backrest adapter plates to mount seat integrated retractors, adjustable backrest inclination.

from the vertical as well, and it incorporates an adapter for mounting seat integrated retractors. An adjustable neck-rest provides support to the ATD-head during the acceleration phase of the sled. The neck-rest also helps to efficiently position the ATD on the aluminum seat with high precision. In addition, a specially designed harness wrapped around the ATD-back and connected to a belt driven safety stop, prevents the ATD from getting damaged when stopping the sled after crash-pulse acceleration by a highly dynamic braking deceleration.

LIMITATIONS AND DISCUSSION

HyDRA® test bench with its RBGI (Figure 12) and T@S (Figure 13) setups are intended to apply a realistic load to the seat belt system up to the beginning of *ride-down* phase, for identifying and validating this most important sequence for innovative seatbelt restraint systems. The ATD like devices are not instrumented for assessing injury values, but for recording precisely the kinematic when they are simultaneously subjected to crash pulses, restrain forces from the SBS, seating surface friction forces, etc…, as well as possible seat belt activation (pretensioning). Once all Digital Twin parameters of the physical HyDRA® test bench are fully derived and identified, the setup kinematics is deemed to be validated, and can be used to gauge the quality of the functional models from which the virtual SBS is build up.

Injury risk assessment is not intended to be done on the physical test bench, but it could be estimated by means of a subsequent full vehicle simulation with Human Body- or ATD-models. The late stage of the ride down phase, where the ATD interacts with the seat and the airbag systems, depends highly on the actual vehicle environment. The deformable passenger seat and other vehicle interior parts for example can significantly influence this late phase. Towards the end of the last in-crash phase, HyDRA®'s ATD kinematic will deviate more and more from the ATD kinematic in a full vehicle setting. The analysis and interpretation of results of the *ride-down* phase from physical tests on the generic bench relative to the in-vehicle behavior would be questionable. Particular effects associated to deformable vehicle seat i.e., "submarining" is not accounted for by the standardized setup and can also not be tested for on a stiff seat bench. Oblique crash scenarios, often encountered in real-world vehicle crashes, often start off with a strong impulse in driving direction followed by growing lateral accelerations as the vehicle is forced into a rotatory motion cannot be represented either. These scenarios cannot be assessed on a one-directional, linear test bench. Also, the two presented simplified ATD kinematics are not geared to predict lateral forces; compared to a biofidelic behavior the pelvis region of HyDRA®'s ATD is per design much stiffer. In all these cases it is more appropriate to assess the occupant dynamics via full scale vehicle simulations with Human Body Models (HBM), with dynamically validated functional seatbelt subsystem models.

CONCLUSION

Reviewing the in-crash phases of classical passive safety a functional segmentation into three distinct phases: *Crash-detection, force-closure* and *ride-down* is appropriate, with the SBS key-functionality to establish *force-closure* of the belt to the vehicle being connected to phase 2. Once *force-closure* is completed the *ride-down* phase with controlled forces in seatbelt and in airbag systems can take over. When transferring this segmentation to integrated safety, phase 1 is transformed to a *pre-crash preparation* phase characterized by significant vehicle ADAS dynamics and /or pre-crash activation of reversible seatbelt systems before a crash event is classified as eminent. The handover to phase 2 is defined by the moment in time, where the irreversible SBS activation is triggered when the SBS-ECU has decided on an imminent crash. This can be either before or after the first physical contact of the ego-vehicle with a bullet vehicle or an obstacle and it is dependent on the quality of the available crash-detection system. The analysis concludes that for Integrated Safety phase 1 and phase 2 cannot be assessed and evaluated individually, as the vehicles and/or SBS pre-crash activation is inseparable linked to the efficient force coupling of the passenger to the vehicle.

The performance of the SBS and its activation is load case i.e., vehicle dependent and can be rated by the single value metric "characteristic shoulder belt force level" illustrated in and discussed following Figure 2. It combines the consumption of safety space and the reduction of kinetic energy on the ATD by a single number: "CLL level".

Most interestingly, by defining a reference vehicle configuration, the *Pretty Good Vehicle* (PGV), and by defining a reference seatbelt system, the *Pretty Good Seatbelt System* (PGS), it becomes possible not only to identify and to rate relative improvements in the seatbelt configuration and in its activation strategy, but also to classify load case scenarios and to optimize on vehicle constellations, provided that the target vehicle does not deviate too much from the PGV.

The presented methodology has the potential to develop and classify a suitable seatbelt system for a target vehicle, and to judge on late changes to the SBS in development program on vehicle level (example different pulse, altered fixation points, …) in a quick and reliable way, without the need of precise information on the passenger seat and on the airbag system used. Potential passenger injury risks for vehicle load cases depend undeniably on the interaction of all system parameters. But when the analyzed SBS with its control strategy performs equally or better than the "gold standard" - *Pretty Good Seatbelt System* – a SBS pre-sign off might help to focus on improving other contributors like seat structures or dashboards, etc.

Using an identical SBS in the target vehicle and the reference vehicle PGV allows to classify the target vehicle. When the target vehicle configuration is rated less advantageous than the PGV, it is from a technical point of view obvious that a more sophisticated SBS, seat, or airbag system is needed to compensate for the deficiency to reach an equivalent safety rating.

Finally, pre-crash scenarios incorporating ADAS or SBS activation can be assessed and rated via the defined metric by the comparison of different activation strategies.

In this paper the derived methodology is presented for the first time in public. Starting from the validated full vehicle simulation model of the PGV the methodology is illustrated via a parameter study applied to this model, and the general application for this methodology is discussed. The test hardware presented in the last section is ready at hand, to validate and backup simulation results assessing vehicle and load case specific SBS qualification including their control strategy. Correlation of physical test data to virtual prediction is beyond the scope of this paper and is first to be revealed in real-world vehicle application projects with our partners in the automotive industry.

OUTLOOK

The prevalent usage of ADAS functionality intend to mitigate or at best avoid an impending crash, utilizing information from outboard sensory systems. The expected earlier classification of an actual driving situation as unavoidable imminent crash will foster the performance and impact of pre-crash activated SBS, although the decision making using environmental sensing still have some challenges to be overcome as described by Straßburger et al. [17]. Pre-crash activated SBSs, including their control strategy, are designed to provide an optimum solution for the momentaneous load case. This will significantly raise the number of elementary load cases to account for during the development process to be eventually only manageable by a virtual approach and efficient coding. Out of the need to assess relevant crash configurations, not addressed by today's regulations or consumer crash tests, virtual assessment methods are required and in development as reported by Dobberstein et al. [18], sharing their standpoint at the EU project OSCCAR. A recently published approach by Schilling et. al. [19] couples MATLAB Simulink to LS-Dyna to describe mechatronic pre-crash activated seat belt systems accurately and efficiently seems promising, and it matches perfectly to the digital twin approach favored by Machens et al. [10].

The simplified setups and the focus to validate the SBS by assuring identical ATD kinematic on the physical and on the digital twin, presented in this paper, intend to broaden this approach, and to be also able to rate the safety benefit of SBS pre-crash activation. The virtual model of the simplified setup with reduced Degrees of Freedom speeds up considerably calculation time and yields in higher numerical stability, making these modes suited for numerical optimization methods, as more variants can be treated in the same amount of time. The ability to validate simulation models on sub-system level for load cases with a seamless transition from low g to high g crash acceleration is seen as a major advantage of the presented device. The results from this paper suggest that the sub-system SBS can be validated and optimized with the HyDRA T@S or - RBGI based on "The Big 8" approach i.e., independent of passenger seat and airbag system. Once the CFL metric is established and widely accepted, the effect of late changes in the vehicle project, which alter the initial "The Big 8" SBS parameter set, can be rated, and evaluated accurately and fast with regards to occupant safety at subsystem level. This performance rating intends to identify suitable SBS more accurately, rather than looking for differences in ATD injury values in a few load cases. In addition, robust results are obtained by using parameter variations in the setup like different lump mass distributions on the ATD to account for occupant diversity.

Reversible pre-crash activation of seatbelt system can start earlier i.e., as soon as the crash detection system has preliminarily identified a rough driving situation or a potential crash event. Belt slack reduction and even occupant repositioning through the SBS can be performed already at moderate forces. Hence reversibility is a major strength of mechatronic SBS. The SBS intervention can be ramped up stepwise according to likelihood of a crash, identified by the crash detection system to provide an optimal occupant protection for the actual driving situation without driver and passenger consciously noticing the intervention. In the joint task to mitigate occupant injury risk seatbelt systems are today already considered as very significant contributor. When developing an adaptive safety functionality, SBS will gain further in importance.

REFERENCES

1. Plankermann, K.," Human Factors as Causes for Road Traffic Accidents in the Sultanate of Oman under Consideration of Road Construction Designs", 2013 Dissertation Universität Regensburg, https://epub.uni-regensburg.de/29768/1/Dissertation%20Kai%20Plankermann.pdf
2. Official Journal of the European Union, L 325/1, 16.12.2019, *EUR-Lex - 32019R2144 - EN - EUR-Lex (europa.eu)*
3. Graci, V., Douglas, E., Seacrist, T., Kerrigan, J., et.al., "Effect of automated versus manual emergency braking on rear seat adult and pediatric occupant precrash motion", Traffic Injury Prevention, Peer-Reviewed Journal for the 26th International Technical Conference on the Enhanced Safety of Vehicles (ESV), 2019, https://doi.org/10.1080/15389588.2019.1630734
4. Schramm, R., "Euro Ncap'S First Step Towards Scenario-Based Assessment By Combining Autonomous Emergency Braking And Autonomous Emergency Steering", Conference: 26th ESV Conference 2019, Endhoven, Paper Number 19-0128, https://www-esv.nhtsa.dot.gov/Proceedings/26/26ESV-000182.pdf
5. NHTSA Announces Update to Historic AEB Commitment by 20 Automakers, https://www.nhtsa.gov/press-releases/nhtsa-announces-update-historic-aeb-commitment-20-automakers, 3.02.2022
6. Spitzhüttl, F., Liers, H.," Calculation of the point of no return (PONR) from real-world accidents", Conference: 26th ESV Conference 2019, Endhoven, Paper Number 19-0141, https://www-esv.nhtsa.dot.gov/Proceedings/26/26ESV-000141.pdf
7. Wågström, K., Leledakis, A., Östh, A. et al.," Integrated safety: Establishing links for a comprehensive virtual tool chain", 26th ESV Conference 2019, Endhoven, Paper Number 19-0177 https://www-esv.nhtsa.dot.gov/Proceedings/26/26ESV-000177.pdf
8. Reuter, R. „Roadmap 2030: Euro NCAP entwickelt neue Kriterien für Crashtests", https://www.automobil-industrie.vogel.de/euro-ncap-entwickelt-neue-kriterien-fuer-crashtests-a-1113849/, 28.04.2022
9. Hu, J., Zhang, K., Reed, M., Wang, J.-W., Neal, M., Lin, C.-H. "Frontal crash simulations using parametric human models representing a diverse population, Traffic Injury Prevention", (2019), 20:sup1, S97-S105, DOI: 10.1080/15389588.2019.1581926
10. Machens, K.-U., Kübler, L.:" Physical & Virtual Dynamic Test-Bench to Approach Integrated Safety", Proceedings Airbag 2022, 15th International Symposium and Exhibition on Sophisticated Car Occupant Safety Systems, 2022, Mannheim, Germany
11. Kramer, F., "Passive Sicherheit von Kraftfahrzeugen." Springer Vieweg, 2009, ISBN 978-3-8348-9254-6.
12. Zellmer, H., Kahler, C., Eickhoff, B.," Optimised pretensioning of the belt system: A rating criterion and the benefit in consumer tests", 19th ESV Conference 2005, Washington, D.C., Paper Number 05-0004, https://www-esv.nhtsa.dot.gov/Proceedings/19/05-0004-O.pdf
13. Voigt, T., Schrenk, W., Zellmer, H., "Enhanced seat belt modelling process to improve predictive accuracy of dummy response in frontal impact", 22nd ESV Conference 2011, Washington, D.C., Paper Number 11-0151, https://www-esv.nhtsa.dot.gov/Proceedings/22/isv7/main.htm
14. Kramer, F., Franz, U., Lorenz, B., Remfrey, J., Schöneburg, R. "Integrale Sicherheit von Kraftfahrzeugen.", 4. Auflage, SpringerVieweg, 2013, ISBN 978-3-8348-2608-4
15. Mages, M., Seyffert, M., Class, U.," Analysis of the pre-crash-benefit of reversible belt pre-pretensioning in different accident scenarios", 22nd ESV Conference 2011, Washington, D.C., Paper Number 11-0442, https://www-esv.nhtsa.dot.gov/Proceedings/22/isv7/main.htm
16. Kuebler, L.; Gargallo, S.; Elsaesser, K.: Characterization and Evaluation of Frontal Crash Pulses with Respect to Occupant Safety, Proceedings Airbag 2008 – 9th International Symposium and Exhibition on Sophisticated Car Occupant Safety Systems, 2008, Karlsruhe, Germany
17. Straßburger, P., Grotz, B., Heiß, S., Arbter, B., Hachmann, K., Metzger, J., Ocelić, N., "Predictive safety: towards holistic top-down systems engineering for pre-crash systems", 27th ESV Conference 2023, Yokohama, Paper Number 23-0234
18. Dobberstein, J., Mayer, C., Kleinbach, C.," Results oft he EU project OSCCAR from Mercedes Benz perspective", VDI-Berichte Nr. 2387, 13. VDI-Tagung Fahrzeugsicherheit, VDI Verlag GmbH Düsseldorf 2022, ISSN 0083-5560, E-ISBN 978-3-18-102387-7
19. Schilling, S., Soni Anurag, Hinrichs H., Verheyen C., Lucht A., Eickhoff B.,"Evaluation of motorized seatbelts in the Euro NCAP AEB-CCFtap scenario: Application of a feedback control loop model in Simulink coupled to a finite element model in LS-Dyna", VDI-Berichte 2387, Proceedings 13. VDI-Tagung Fahrzeugsicherheit, VDI Verlag GmbH Düsseldorf 2022, E-ISBN 978-3-18-102387-7
20. Regulation No 16 of the Economic Commission for Europe of the United Nations (UNECE) Supplement 2 to the 07 series of amendments — Date of entry into force: 19 July 2018, Official Journal of the European Union 27.4.2018, page L 109/1-99 http://www.unece.org/trans/main/wp29/wp29wgs/wp29gen/wp29fdocstts.html

CONTACT INFORMATION

Dr.-Ing. Kai-Ulrich Machens, Manager SBS Core Engineering, Test Methodology & Acoustics, ZF Automotive Germany GmbH.
Email : kai-ulrich.machens@zf.com ; phone: +49 7172 302-2286

Dr.-Ing. Lars Kübler, Director SBS Core Engineering, ZF Automotive Germany GmbH.
Email : lars.kuebler@zf.com ; phone: +49 7172 302-2230

ACKNOWLEDGMENTS

This work gained from the helpful discussions and substantial contributions from various colleagues at ZF Automotive Germany GmbH, Alfdorf Germany. The authors would like to thank Dr. Matthias Bier, Milos Cekic, Steffen Dambacher, Adrian Landbeck, Michael Stegmeier for their contributions to this paper. The new test equipment was designed within a test bench development project including the support from external partners. The authors would like to thank the entire HyDRA® project team especially Dr. Bartholomäus Brylka, Lukas Hagmanns, Jürgen Hirth (all ZF Automotive Germany GmbH) and Dr. Andreas Rieser, Patrick Mayrhofer (both Humanetics Austria GmbH) for their passion and contributions to the development of the bench. Additional thanks go to Dr. Jens Neumann and Andrea Weiss (both ZF Automotive Germany GmbH) for LS-DYNA simulation to develop the SBS *force-closure* performance criterium. Special thanks go to Dr. Jens Scholz (ZF Automotive Germany GmbH) for extensive proof reading and his care for better text comprehensibility.

APPENDIX A

Evaluation from full vehicle to equivalent bench setup

A validated full vehicle safety system simulation model is best suited to study the effects of model reduction. In contrast to physical tests, it shows no variability in terms initial and boundary conditions, i.e., ATD seating position, belt routing and slack, etc. Sensitivity analyses with this "full safety system" (FSS) model are used to evaluate the effect of model simplifications on kinematics and forces characterizing the ATD dynamics. Figure 14 illustrates this process by means of four basic vehicle environments derived from a midsize sedan with a 5-star rating in current U.S. NCAP as reference vehicle, designated *Pretty Good Vehicle* (PGV). The safety system of the FSS consist of a Switchable Load Limiter (SLL) switching the shoulder belt force from 5 kN to 3 kN at 62 ms and a passenger airbag, the other three configurations are equipped with a retractor-pretensioner and a constant load limiter (CLL) with 5 kN shoulder force and no airbag.

All setups are equally subjected to US NCAP pulse of the PGV for Full Width Frontal Impact (FWFI) at 56 km/h (designated as load case LC0) starting with an H350 ATD model seated on the front passenger seat. The four configurations from Figure 14 show the model complexity is stepwise reduced, from (A) full vehicle SBS, (B) airbags removed, (C) vehicle seat replaced by steel seat and finally (D) ATD arms replaced by lump masses of 3 kg and the under legs substituted by a hinged gear with a 1 kN-damper. The dynamic response of the ATD is described by the three force / displacement pairs displayed in Figure 15: at the retractor; retractor force / webbing pay-out, at the upper body; shoulder belt force / chest forward displacement, and at the lower body; anchor belt force / tongue slip.

Figure 14 (A) Validated full safety system (FSS) from a midsize sedan (PGV) with (left picture, result in Figure 15: black continuous line) and (B) without airbag system (center left picture, result: black dashed line) is transferred to a configuration with identical anchor point geometry, same H350 (H-angle) (C) but seated on a steal seat with a seating surface tilted by 10° and fixed foot rest position as in FSS (center right picture, result: green dotted line). (D) Simplified bench test setup called "Torso at seat" (T@S) with under legs replaced by a hinged stiff gear and a viscous 1 kN damper, H350 arms substituted by lumped masses of 3 kg fitted to the shoulder hinges (right picture, result: green continuous line).

In phase 1 and 2 the full vehicle configuration and steel seat correlate well for retractor and for the ATD upper body, they diverge only for the anchor belt force. The linear damper at the shank in setup D reduces the anchor belt force in comparison to setup C, but it is not able to cover all effects starting from sliding feet pulling on the tibia up to the feet encountering an obstacle resulting in a complex motion and force sequence. However, the anchor belt force matches in phase 2 adequately with the FSS. The largest deviation in anchor belt force results from the significant restraint performance of the deformable passenger seat at about 70 ms, when the ATD buttocks dives into the seat, causing large contact forces. Fortunately, this effect occurs in phase 3 and hence the simplified setup called Torso @ Seat (T@S) (green continuous line) is able to predict phase 1-2 accurately and independently from the real passenger seat. However, it should be emphasized, that the absolute characteristic force level calculated by using a constant load limiting level to stop the chest forward displacement from T@S configuration at 300 mm is influenced by the lower leg damper characteristics, since the damper dissipate energy from the system, intended like a real vehicle seat.

When comparing the horizontal shear forces acting on the *collarbone* with ATD arms and with lump mass substitutes, shown in Figure 16, it can be concluded that 3 kg lump masses, attached to the shoulders of T@S-ATD represent adequately the dynamic interaction of ATD arms to the torso. As replacing the ATD arms does hardly alter the ATD dynamics in phase 1 and 2, the ATD with lump masses is considered an adequate representation of an H350-ATD. Also, the variant with lump mass improves on test setup repeatability, and prevents damage from uncontrolled moving arms during the test.

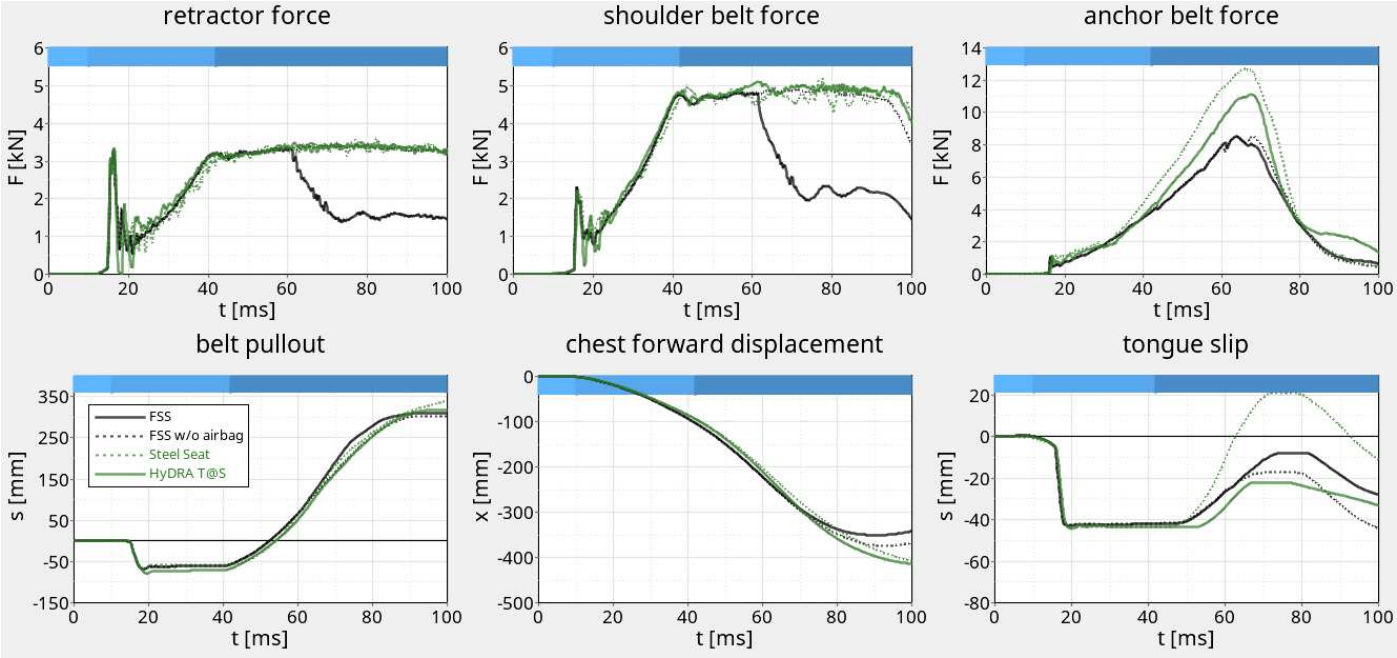

Figure 15 Dynamic ATD response (PGV subjected to LC0: US NCAP pulse for FWFI at 56 km/h with an H350 ATD) for four configurations with stepwise reduced complexity presented in Figure 14 (including scenario associated colors / style definition) expressed by force/displacement pairs for pretensioner, for upper and for lower body. The color banner above the graph differentiates between the in-crash phases 1-3. Comparable results prior to force-closure for all measures except the pelvis force. The misfit (green dotted line) results from low steel seat friction, which is in the final reduction step compensated by a damper added to the hinged gear system substituting the ATD legs (green continuous line).

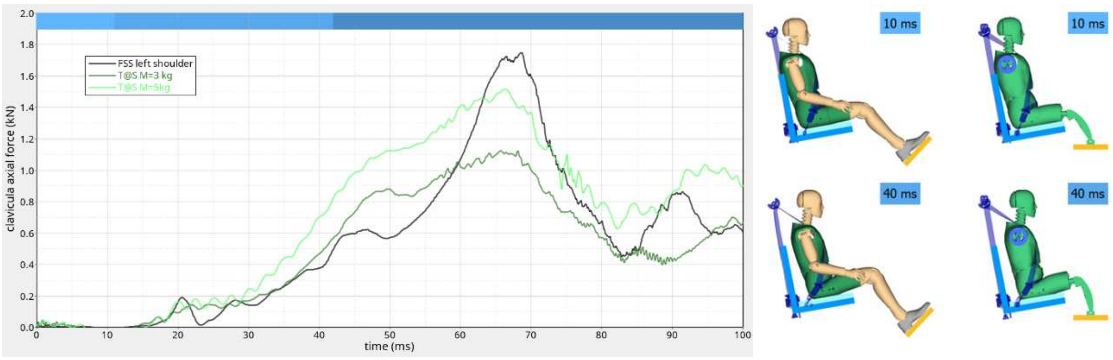

Figure 16 Comparing the horizontal shear force in the left collarbone for the FSS configuration with H350-ATD arms (black line) to its shear force in T@S configuration with lump masses of M=5 kg (light green line) and M=3 kg (dark green line) substitute identifies 3 kg as adequate dynamical replacement. Left picture: Both ATD kinematics shows good agreement for example at the begin of in-crash phase 1 and at the begin of phase 2.

Sensitivity to configuration parameters

Baseline for this investigation is the simplified bench test setup D.0 as presented in the previous section. Figure 17 depicts the different parameters analyzed: D.1: pelvis slack (40 mm added at anchor), D.2: backrest orientation steeper by 5°, D.3: fixation points (anchor and buckle moved by 100 mm to rear) and D.4: D-ring position shifted by 200 mm to rear. The corresponding dynamic ATD responses are displayed in Figure 18.

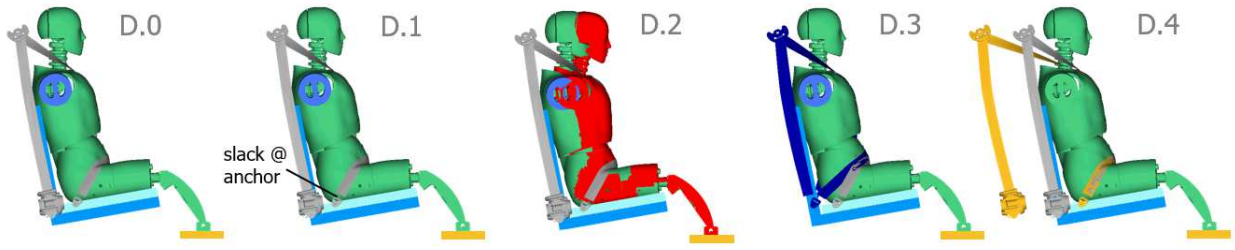

Figure 17 Illustration of four single parameter variations on the simplified bench test setup (D.0) from Figure 15 (from left to right) by D.1: adding 40 mm belt slack at the anchor, D.2: backrest rotated by 5° to the vertical, D.3: anchor and buckle fixation points moved 100 mm to the rear, D.4: D-Ring fixation moved 200 mm to the rear.

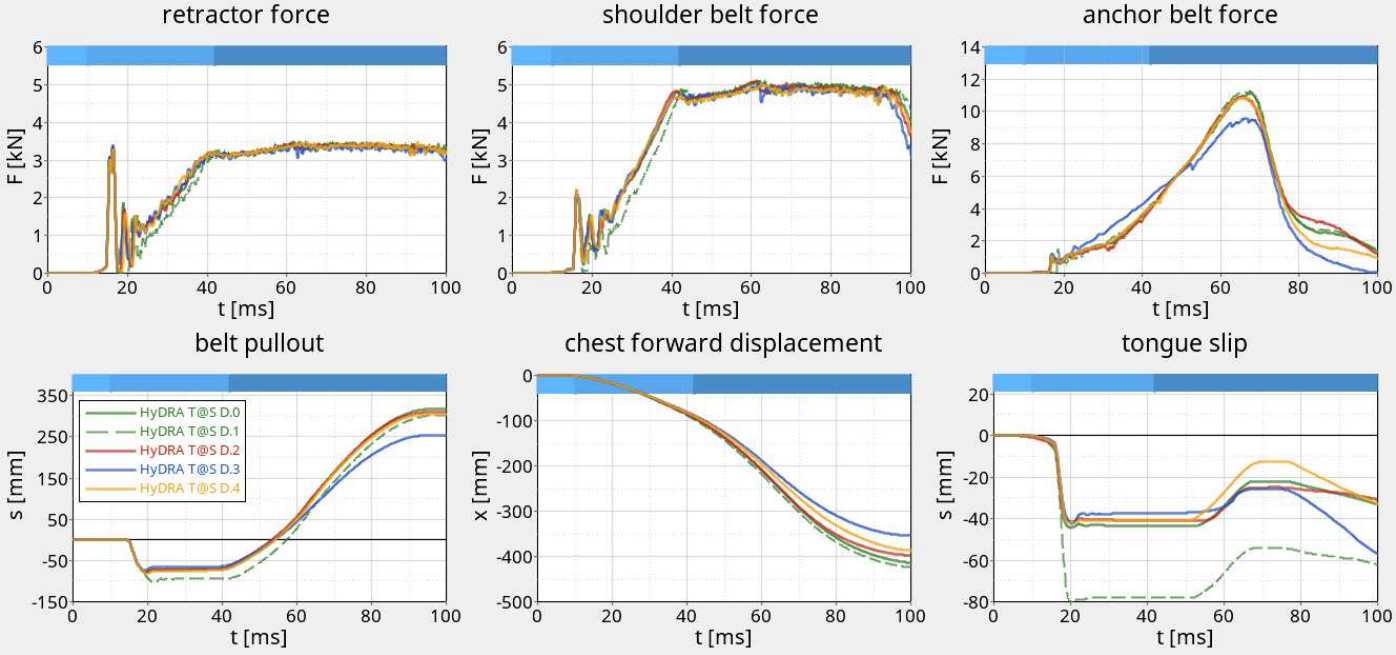

Figure 18 Dynamic ATD response (subjected to LC0: US NCAP pulse of the PGV for FWFI at 56 km/h with an H350 ATD) for the baseline and four single parameter variations. The added pelvis slack hidden in D.1 (dashed line) at the end of the belt is not fully absorbed by the larger pretensioner pull-in. The changes in the belt geometry D.2-D.4 are not visible in retractor and shoulder force neither in belt pull-in but affect the chest forward displacement.

The added 40 mm belt slack in D.1, being a significant amount of slack, introduced at the anchor furthest away from the retractor pretensioner is not fully compensated by extra pretensioner pull-in, consequently it affects the ATD chest forward displacement. Modifying the ATD initial condition to a 5° more upright seating position (D.2), as well as modifying the webbing orientation at the fixation points (D.3 and D.4) do not significantly affect the force vs. time behavior. However, the altered belt inclination from ATD to SBS fixation change the force vector in driving direction and sum up to significant differences in the displacements. Chest forward displacement and retractor belt pull-out are closely correlated whilst tongue-slip is less predictive, as it is more sensitive to the changed ATD pelvis kinematic.

The configuration D.3, resulting in the shortest maximal chest forward displacement differs in anchor force vs. time behavior from the other configurations in Figure 18. The changed webbing orientation, predominantly in the lap belt, is assumed to be responsible for a faster slack removal in the pelvis region by the natural pelvis forward displacement, such that pelvis belt forces and friction forces between seating surface and ATD become larger. Therefore, the higher forces acting between seating surface and ATD buttocks restrain the pelvis region. Particularly the changed belt pull-out characteristics of configuration D.3 indicates that the ATD kinematics has been changed, which might influence the ratio of shoulder belt force to energy present in the ATD, as discussed in Appendix B. Consequently, a comparison via CFL of kinematically different configurations like D.3 might be biased.

An analogous kinematic consideration can be applied to configuration D.2 and D.4. Both show a belt routing from ATD to fixation points that are directed more to the rear, and consequently both yield in reduced chest forward displacements. These geometric effects are expected to be perfectly captured by simulation models.

The chest deflection results from this parameter study are displayed in Figure 19, comparing chest deflection for a fixed CLL level in the upper row and different CLL levels (Characteristic shoulder force level – CFL) in the lower row, so that the different configurations yield the same maximal chest forward displacement of 300 mm. Maximal chest deflection is linked to injury assessment ratings like in EU NCAP and it is used as protection criteria for frontal impact in legal requirements. The smallest maximal chest deflection for equal shoulder belt forces and for equal maximum forward displacement is achieved with D.4. The different belt rooting may also contribute to this result, as the belt might be routed further away from the chest deflection sensor point, or closer to the stiff “non biofidelic” clavicle of the H350 ATD deflecting the belt more, thereby reducing the amount of the shoulder belt forces and compressing the chest. Gauging these effects for real-world safety, the ranking deduced from the characteristic shoulder force level reported in

Table 1, the configuration D.3 comes out best, followed by D.4 and D.2. When analyzing the systems with respect to maximal chest deflection with equal maximum chest forward displacement, as illustrated in the lower row of Figure 19, configuration D.4 and D.3 are comparable followed by D.2. D.1 is rated less preferable than D.0.

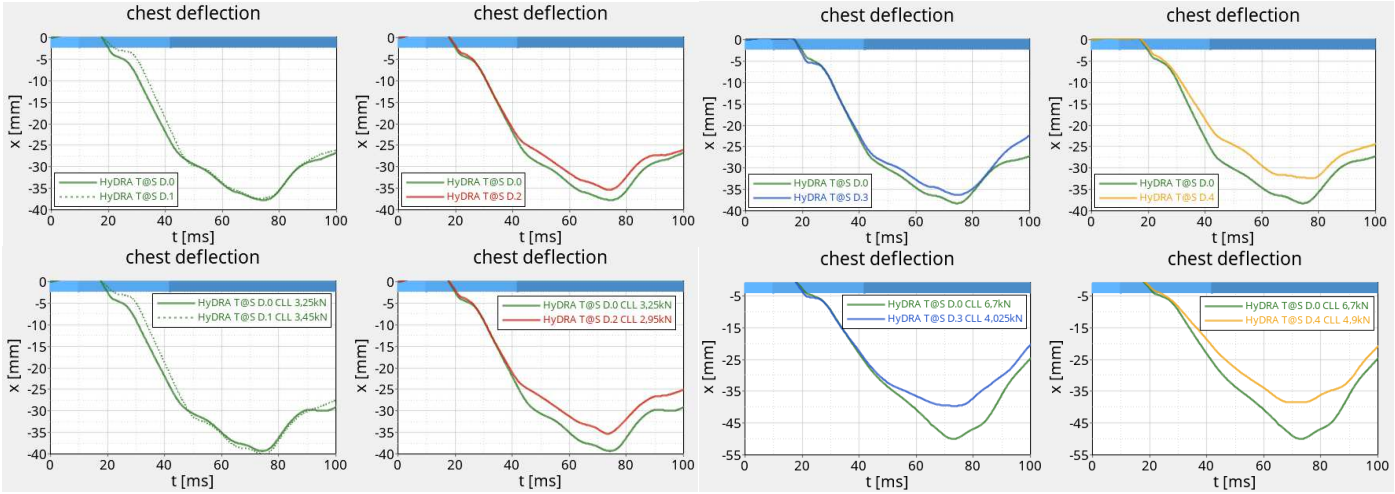

Figure 19 First row: Chest deflection results for the parameter study with configurations in Figure 17 D.1, D.2, D.3, D.4 are compared from left to right with the baseline D.0. The baseline D.0 (apart from D.1 with added slack) remarkably combines largest chest deflections with largest chest forward displacement. Second row: Chest deflection by using the characteristic shoulder force CFL as CLL level, resulting in an identical maximal chest forward displacement in all configurations.

APPENDIX B

Energy Considerations for CFL with maximal chest forward displacement set to 300 mm

The quantity *characteristic shoulder force level* (CFL) introduced and illustrated in Figure 2 is linked to a maximal chest forward displacement distance offset, set to 300 *mm*, and this quantity coincides with the dynamic test requirement for UNECE regulation R16 [20] to homologate standalone seatbelt systems. The CFL is per definition the *constant* force level needed to stop the ATD chest forward displacement over the *remaining* length, i.e., 300 mm minus the displacement already consumed for *force-closure*. During the *ride-down* phase the ATD kinematics is almost predictable. The pelvis forward displacement is stopped around t=67 ms, coinciding with the maximum peak in the anchor belt force. The maximum chest deflection, regarded as most relevant injury risk quantity, directly associated to seatbelt action, occurs shortly after this point in time (see Figure 19), as the stopped hip introduces an angular moment to the upper body, rotating around the hip joint. Herein the mechanical chest impedance of the ATDs skin vest-foam-rib arrangement, identified by Machens et. al. [10] (in Appendix A Figure 8) to correspond to a mass-spring-damper system with a natural frequency of about 66 Hz, accounts for a delay of 4 ms before a maximum normal chest force results in a maximum chest deflection.

The magnitude of the normal chest force caused by the belt depends on the distance of the routed belt to the chest displacement sensor as well as on the friction coefficient between chest and belt. A rough estimate of typical vehicle configurations in [10] indicates, that less than 50% of the shoulder belt force is directed normal to the chest. This ratio depends on the bend angle of belt around the shoulder, namely on the direction the belt is leaving the shoulder to the D-ring. This should be kept in mind, when directly comparing characteristic shoulder force levels (CFL) from different vehicle configurations i.e., for example changed seating or backrest positions or changes in D-ring positions.

The shoulder belt force, apart from the fact of causing chest deflection, is of major importance to limit the chest forward displacement by dissipating the energy stored in the system. In a system without airbags, ATD energy is presumably dissipated to a minor degree by seat friction, but mainly by shoulder belt force. The work carried out by the shoulder belt force can be calculated by multiplying it with the shoulder belt displacement i.e., belt pull-out from the D-ring.

In most real-world safety systems, the frontal airbag takes over presumably before 300 mm chest forward displacement to trap as soft as possible the upper body and head of the occupant. Therefore, the introduced quantity CFL shoulder force levels are logically significantly higher as the ones observed in actual safety systems with airbags. CFL should be simply regarded as metric, not as meaningful physical quantity for seatbelt systems. This becomes apparent when transferring SBS-1 and SBS-2, both in full vehicle environment using a CLL system (shoulder belt force 5000 N), to a system without airbags. For load case LC0 in Figure 5 both systems stop the chest forward displacement of the T@S slightly beyond 400 mm (SBS-1: 416 mm, SBS-2: 410 mm). In order to stop the ATD at 300 *mm* maximum chest forward displacement CFL of 10000N (SBS-1) and 8800 N (SBS-2) respectively are required, see Table 2.

It is interesting to compare and discuss these results. In Figure 20 the simulation results for shoulder belt force and *shoulder belt displacement* (i.e., pull-out from the D-ring) for SBS-1 (green) and SBS-2 (blue) are shown for load limiting with different CFL (continuous line) and for identical CLL (dashed line). For same CLL levels (dashed line) the more efficient SBS-2 (larger belt pull-in, no locking dip) reaches *force-closure* (see Figure 20 upper left picture) about 3 *ms* earlier than SBS-1 but features an similar shoulder belt displacement *after* locking (see Figure 20 lower right picture, small difference may be related to differences in pretensioner design), revealing that the integral from shoulder belt force over shoulder belt displacement (see Figure 20 lower

left picture) and hence the work executed by both systems to stop the chest forward displacement is very similar. Both systems need the same time and displacement to stop chest forward displacement *after* locking and therefore is the difference of 6 mm in maximum chest forward displacement visible in Figure 5 (SBS-2: 410 mm, SBS-1: 416 mm) resulting from a larger belt pull-in of SBS-2, 98 mm compared to 72 mm for SBS-1.

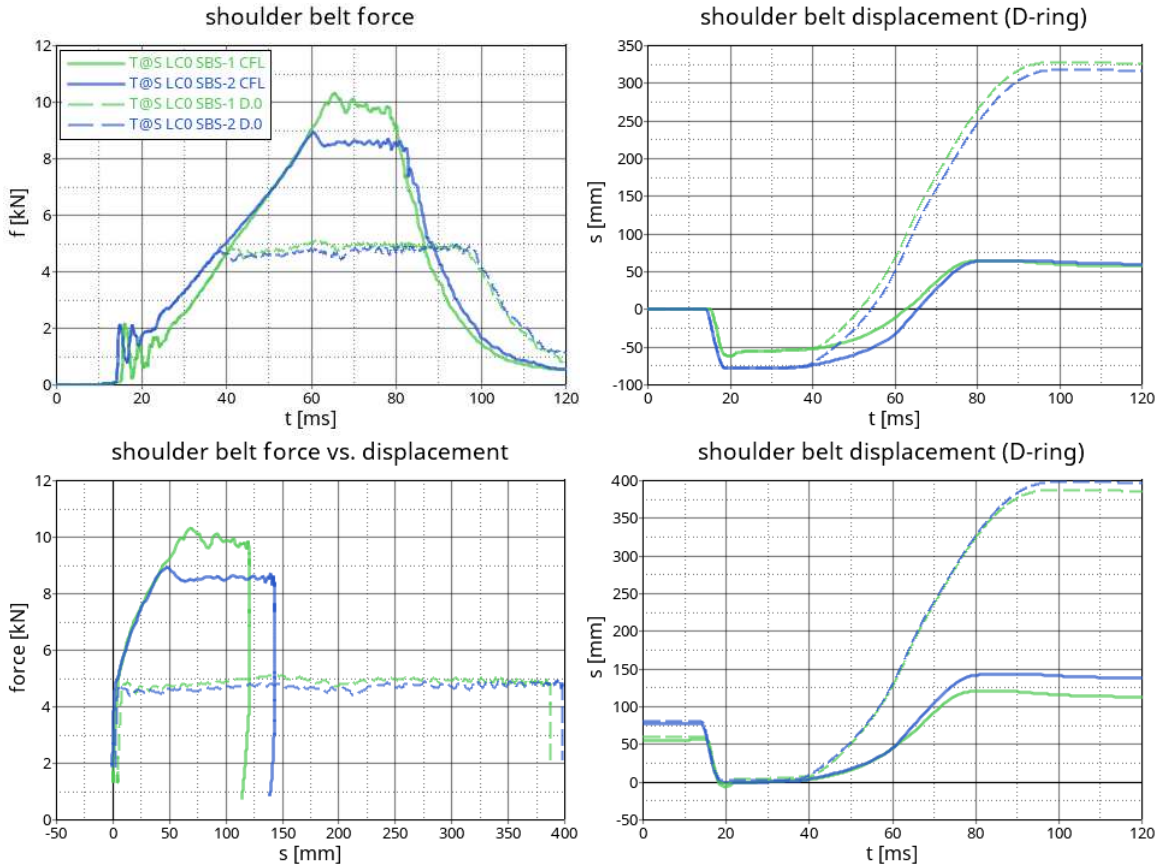

Figure 20 Dynamic T@S response when subjected to LC0 for two different SBSs as in Figure 5: SBS-1 (green) and SBS-2 (blue) with equal CLL (dashed line) and with individual CFL (continuous line). Displaying shoulder belt force vs time (upper left picture), shoulder belt displacement after crash start (t=0) (upper right picture) and after locking (t=22 ms) (lower right picture), shoulder belt force vs. shoulder belt displacement after locking (lower left picture). Shoulder belt displacement after locking is almost equal for same CLL level and different for different CFL, while equal shoulder belt displacement after crash start is observed for same CFLs. Amount of dissipated energy for lower CFL of SBS-2 multiplied by a larger distance similar as the higher CFL of SBS-1 over shorter distance as integral of the over shoulder belt force vs. displacement represents work done by shoulder belt force. Identical force onset for SBS-1 and SBS-2 point to exclusive crash pulse influence (lower left picture).

Limiting the maximum chest forward displacement to 300 mm as defined by the CFL metric is almost equivalent to limit the absolute shoulder belt displacement to 64 mm (at t=80 ms) visible in Figure 20 (upper left picture). The gain in belt pull-in after retractor locking (at t=22 ms), which amounts to a total difference of 22 mm (SBS-2: -78 mm, SBS-1: -56 mm) in shoulder belt displacement is fully used to extend this displacement in the load-limiting phase (Figure 20 lower left picture: SBS-2: 142 mm, SBS-1: 120 mm). To dissipate the same amount of energy with less shoulder belt displacement the characteristic force level needs to be higher for SBS-1. The CFL is almost the ratio of energy (work of the shoulder belt force), needed to stop chest forward displacement at 300 mm, to the rest shoulder belt displacement (available after force-closure) and therefore combines both quantities meaningful for the scenario under investigation.

The relative benefit of the saved shoulder belt displacement to the available *rest* displacement after *force-closure* naturally depends on specified maximum chest forward displacement distance. Referring to Table 2, SBS-1 is for T@S LC0 13.6% less favorable than SBS-2. If 400 mm instead of 300 mm would have been defined as limit to calculate the characteristic shoulder force level, a CFL* of 5200 N (SBS-1) and 4900 N (SBS-2) would be obtained, which corresponds to a disadvantage of only 6% for SBS-1 respectively SBS-2 (PGS). CFL based on 300 mm maximum chest forward displacement is deemed suitable to distinguish the performance of seatbelt systems in a meaningful way, as it reflects reasonably well average vehicle configurations on the market, and also reflects the UNECE R16 homologation requirement.